Atmospheric
Chemistry
and Physics
Discussions

Open Access

Chemical characterization and source apportionment of PM$_{2.5}$ in Beijing: seasonal perspective

R. Zhang[1,*], J. Jing[1,2], J. Tao[3], S.-C. Hsu[4], G. Wang[5], J. Cao[5], C. S. L. Lee[6], L. Zhu[3], Z. Chen[7], and Y. Zhao[7]

[1]Key Laboratory of Regional Climate-Environment Research for Temperate East Asia, Institute of Atmospheric Physics, Chinese Academy of Sciences, Beijing
[2]University of Chinese Academy of Sciences, Beijing
[3]South China Institute of Environmental Sciences, Ministry of Environmental Protection, Guangzhou
[4]Research Center for Environmental Changes, Academia Sinica, Taipei
[5]K LAST, SKLLQG, Institute of Earth Environment, Chinese Academy of Sciences, Xi'an
[6]Institute of Earth Sciences, Academia Sinica, Taipei
[7]ESPC, College of Environmental Sciences and Engineering, Peking University, Beijing
[*]The first four authors have equal contributions to the paper.

Discussion Paper | Discussion Paper | Discussion Paper | Discussion Paper

ACPD

13, 9953–10007, 2013

Chemical characterization and source apportionment

R. Zhang et al.

Title Page

Abstract | Introduction

Conclusions | References

Tables | Figures

|◄ | ►|

◄ | ►

Back | Close

Full Screen / Esc

Printer-friendly Version

Interactive Discussion

Title Page

Abstract | Introduction

Conclusions | References

Tables | Figures

◄ | ►

◄ | ►

Back | Close

Full Screen / Esc

Printer-friendly Version

Interactive Discussion

Abstract

In this study, 121 daily $PM_{2.5}$ (aerosol particle with aerodynamic diameter less than 2.5 µm) samples were collected from an urban site in Beijing in four months between April 2009 and January 2010 representing the four seasons. The samples were de-termined for various compositions, including elements, ions, and organic/elemental carbon. Various approaches, such as chemical mass balance, positive matrix factor-ization (PMF), trajectory clustering, and potential source contribution function (PSCF), were employed for characterizing aerosol speciation, identifying likely sources, and apportioning contributions from each likely source. Our results have shown distinc-tive seasonalities for various aerosol speciations associated with $PM_{2.5}$ in Beijing. Soil dust waxes in the spring and wanes in the summer. Regarding the secondary aerosol components, inorganic and organic species may behave in different manners. The for-mer preferentially forms in the hot and humid summer via photochemical reactions, al-though their precursor gases, such as SO_2 and NO_x, are emitted much more in winter. The latter seems to favorably form in the cold and dry winter. Synoptic meteorological and climate conditions can overwhelm the emission pattern in the formation of sec-ondary aerosols. The PMF model identified six main sources: soil dust, coal combus-tion, biomass burning, traffic and waste incineration emission, industrial pollution, and secondary inorganic aerosol. Each of these sources has an annual mean contribution of 16, 14, 13, 3, 28, and 26 %, respectively, to $PM_{2.5}$. However, the relative contributions of these identified sources significantly vary with changing seasons. The results of tra-jectory clustering and the PSCF method demonstrated that regional sources could be crucial contributors to PM pollution in Beijing. In conclusion, we have unraveled some complex aspects of the pollution sources and formation processes of $PM_{2.5}$ in Bei-jing. To our knowledge, this study is the first systematical study that comprehensively explores the chemical characterizations and source apportionments of $PM_{2.5}$ aerosol speciation in Beijing by applying multiple approaches based on a completely seasonal perspective.

Title Page

Abstract | Introduction

Conclusions | References

Tables | Figures

◄ | ►

◄ | ►

Back | Close

Full Screen / Esc

Printer-friendly Version

Interactive Discussion

1   Introduction

Particulate matter (PM) is composed of various chemical components (Seinfeld, 1989). PM profoundly affects our living environments in terms of air quality (in close relation to public health), visibility, direct and indirect radiative forcing, climate effects and ecosystems (Watson, 2003; Streets et al., 2006; Andreae and Rosenfeld, 2008; Mahowald, 2011). Numerous epidemiological studies have demonstrated that longterm exposure to pronounced $PM_{2.5}$ increases morbidity and mortality (Dockery and Pope, 1995; Pope et al., 1995; Schwartz et al., 1996). Given its tiny size, fine mode PM (i.e. $PM_{2.5}$, PM with aerodynamic diameter less than 2.5 μm) can readily penetrate the human bronchus and lung (Pope et al., 1995; Oberdorster, 2001). Through absorption and scattering of solar radiation and serving as cloud condensation nuclei, $PM_{2.5}$ extensively affects the global climate (Bardouki et al., 2003), and thus, the hydrological cycle (Ramanathan and Feng, 2009). The diverse effects of $PM_{2.5}$ could be a function of its complex chemical components and composition (He et al., 2009; Niwa et al., 2007; Malm et al., 2005; Eatough et al., 2006).

Due to the rapid economic and industrial developments and urbanization in the past few decades, there is an escalating increase in energy consumption and the number of motor vehicles in China, where air pollution has become ubiquitous (Chan and Yao, 2008). According to Shao et al. (2006), nearly 70 % of urban areas in China do not meet China's national ambient air quality standards, which are even much laxer than the air quality exposure standards/guidelines of the World Health Organization (WHO, 2005). The Beijing–Tianjin–Hebei region, the Yangtze River Delta, and the Pearl River Delta are of special concern because of their severe PM pollution, which can be explicitly shown by the spatial distribution of aerosol optical depth (AOD) retrieved by satellites (He et al., 2009; Lee et al., 2010). Three megacities that are representatives of each region, namely, Beijing, Shanghai, and Guangzhou, are the foci, because of their dense population. Coal is the primary energy source in China, and its consumption reached up to 1528 Mtce in 2005, accounting for nearly 70 % of the total energy consumption

Chemical characterization and source apportionment

R. Zhang et al.

(followed by petroleum at over 20 %). Such quantity ranks number one in the world, representing ∼ 37 % of global consumption (Fang et al., 2009; Chen et al., 2010). The use of coal in China encompass from large power plants, industries to individual domestic households where coal combustion is the largest contributor of air pollution (Liu and Diamond, 2005; Chan and Yao, 2008). Given the rapid growth in vehicle numbers at a rising rate of ∼ 20 %, traffic has become a major urban pollutant emitter (He et al., 2002; Fan et al., 2009). Other than anthropogenic pollutants, desert and loess dust of natural origins with annual emissions of over 100 million tons also serves as important PM source in China, particularly in late winter and spring (Zhang et al., 1997; Sun et al., 2001).

Atmospheric pollutants in China are a complex mixtures of various sources, from gases to particulates, from natural to anthropogenic, from primary to secondary, and from local to regional and the term "Air Pollution Complex" or "Complex Atmospheric Pollution" has been emerged in the last decade (He et al., 2002; Shao et al., 2006; Chan and Yao, 2008; Fan et al., 2009). One of the major air pollutants is PM, particularly $PM_{2.5}$, which remains a nationwide problem despite considerable efforts for its removal (Fan et al., 2009). As the capital of China and a rapidly industrialized and typical urbanized city, Beijing has elicited much more attention domestically and internationally (Zhang et al., 2003a, 2007; Zhou et al., 2012). $PM_{2.5}$ in Beijing is abnormally elevated, often rising to more than $100 \, \mu g \, m^{-3}$, and characterized by multiple components and sources, ranging from inorganic to organic constituents, from anthropogenic to natural origins, from primary to secondary components, and from local to long-range transported sources, and in dynamic variability with time and/or meteorological conditions and climate regimes (He et al., 2001; Wang et al., 2005; Duan et al., 2006; Okuda et al., 2011; Song et al., 2012). In spite of many scientific research programs conducted by academic institutions and the political strategies implemented by the government, the state of air pollution in Beijing (and even across China) seems to improve slowly. For instance, in January 2013, Beijing (and the entire inland China) suffered from the worst $PM_{2.5}$ pollution in history, registering

the highest PM$_{2.5}$ hourly concentration of 886 µg m^{-3} (http://www.nasa.gov/multimedia/
imagegallery/image_feature_2425.html). Some essential questions remain unknown,
although the government has devoted itself to improving air quality and numerous stud-
ies have been conducted. Therefore, a systematically comprehensive investigation of
5 employing multiple techniques in conjunction with chemical measurements is inevitably
needed, particularly to unravel the likely contributors of PM$_{2.5}$.

Receptor models are used to quantitatively estimate the pollutant levels contributed
by different sources through statistical interpretation of ambient measurement. The
positive matrix factorization (PMF) developed by the Environmental Protection Agency
10 of USA is a well adopted receptor model for source apportionment analysis. A few
studies have applied PMF to identify the likely dominant sources and apportion their
respective contributions. For example, Wang et al. (2008) analyzed certain elements,
ions, and black carbon in PM$_{2.5}$ and PM$_{10}$ samples collected in Beijing in summer and
winter (one month representative for each season) between 2001 and 2006. Based on
15 the obtained data set, they performed PMF analyses and identified six main sources:
soil dust, vehicular emission, coal combustion, secondary aerosol, industrial emission,
and biomass burning. By applying the PMF model with only elemental data as input
data, Yu et al. (2013) identified seven likely sources of PM$_{2.5}$ in Beijing, with relative
contributions following the order secondary sulfur (26.5 %), vehicle exhaust (17.1 %),
20 fossil fuel combustion (16. %), road dust (12.7 %), biomass burning (11.2 %), soil dust
(10.4 %), and metal processing (6.0 %). Song et al. (2007) analyzed a few elements,
ions, and organic/elemental carbon (OC/EC) in PM$_{2.5}$ collected from multiple stations in
Beijing during a short period in January and August 2004, and subjected them to PMF
analyses. Six potential sources were registered: coal combustion, biomass burning,
25 secondary sulfate, motor vehicles, secondary nitrate, and road dust, with emphases on
coal combustion in winter and secondary aerosols in summer. Xie et al. (2008) con-
ducted PMF analyses of PM$_{10}$ (instead of PM$_{2.5}$) collected in Beijing in 10 days each in
January, April, July, and October 2004 by using chemical data on metal elements, ions,
and OC/EC as input data. Seven main sources were identified, including urban fugitive

dust, crustal soil, coal combustion, secondary sulfate, secondary nitrate, biomass burning with municipal incineration, and vehicle emissions. All these studies were limited to a particular season and based on selected PM species.

To attain a better understanding of the chemical characteristics and sources of fine aerosols on a seasonal basis, we conducted a delicate investigation in Beijing. We continuously collected daily $PM_{2.5}$ samples at an urban site for four months, each of which in the respective seasons (i.e. spring, summer, autumn and winter). The samples were subjected to chemical measurements of various aerosol compositions as a whole, such as a suite of crustal and anthropogenic elements, major water-soluble ions, and OC/EC. Furthermore, we identified and apportioned the main sources to $PM_{2.5}$ by employing chemical mass closure construction and the PMF model in conjunction with trajectory cluster and potential source contribution function analyses according to the hybrid singleparticle Lagrangian integrated trajectory (HYSPLIT) model. This study will elucidate the source profile of $PM_{2.5}$ in different seasons and the relative contribution from each source in the complex urban airshed in Beijing and provide vital information in formulating the future air management framework to address the current alarming level of PM pollution in China which has been affecting the air quality on a vast regional scale.

2   Methodology

2.1   Sample and chemical analysis

2.1.1   Sampling site

Beijing is located on the northern edge of the North China Plain, surrounded by the Yanshan Mountains in the west, north, and northeast (Fig. 1). According to the spatial distribution of fine AOD ranging from 0.0 to 1.0 that has been retrieved from Moderate-resolution Imaging Spectrometer (MODIS) sensors on board Terra and Aqua satellites

(Fig. 1), Beijing is one of the PM$_{2.5}$ hot spots in China. The four seasons are characterized by variable meteorological conditions: spring by highspeed winds and low rainfall, summer by high temperature and frequent rain usually accounting for 75 % of annual rainfall, autumn by sunny days and northwest winds, and winter by cold and dry air. The population is 17.55 million. In 2009, the number of motor vehicles increased to 4.019 million, and energy consumption was equivalent to 65.73 million tons of standard coal (Beijing Statistics Yearbook, 2010). The sampling station was set up at the roof of the Science Building in Peking University (116.30° E, 39.99° N) 26 m a.g.l. A few field experimental campaigns have been conducted at this urban site (He et al., 2010; Guo et al., 2012). This site is located within the educational, commercial, and residential districts, and no main pollution sources exist nearby. Thus, the observations could be typical of the general urban pollution in Beijing.

2.1.2 Sample collection

Daily PM$_{2.5}$ samples were collected in April, July, and October 2009 and January 2010, representing spring, summer, autumn, and winter, respectively. Two collocated aerosol samplers (frmOMNI^{TM}, BGI, USA) were used to collect PM$_{2.5}$ samples from 10 a.m. to 10 a.m. the next day simultaneously. The two substrates used in each sampler were 47 mm quartz filter (Whatman QM/A, England) and Teflon filter (pore size = 2 µm; Whatman PTFE, England). The flow rate was set at 5 L min^{-1}. The quartz filters were baked at 800 °C for 3 h before use. The filter samples were stored at −18 °C until pretreatment.

2.1.3 Gravimetric weighing

Before and after each sampling, the PTFE filters were conditioned at 22 ± 1 °C in relative humidity of 35 ± 2 % for 24 h and then weighed in a weighing room by using an electronic balance with a detection limit of 1 µg (Sartorius, Gottingen, Germany). The corresponding PM$_{2.5}$ mass concentration of each filter was equal to the weight difference before and after sampling divided by the sampled air volume.

2.1.4 Chemical analysis of trace elements and water-soluble ions

Prior to extraction and digestion, each aerosol-laden PTFE membrane filter was cut into two equal halves with ceramic scissors. One half was subjected to Milli-Q water extraction for ionic measurement and the other half to acid digestion for elemental measurement. For the acid digestion, the polypropylene support O-ring on half of each PTFE filter sample was carefully removed with a ceramic knife from contamination. The filter samples were digested with an acid mixture ($5\,\text{mL HNO}_3 + 2\,\text{mL HF}$) by using an ultra-high throughout microwave digestion system (MARSXpress, CEM, Matthews, NC). A blank reagent and two filter blanks were prepared in each run following the same procedure used for the samples. All the acids used in this study were of ultra-pure grade (Merck, Germany). The detailed digestion method has been published elsewhere (Hsu et al., 2008). Another half of all filter samples were used for extraction with 20 mL Milli-Q purified water (specific resistivity = $18.2\,\text{M}\Omega\,\text{cm}$; Millipore, Massachusetts, USA) for 1 h. The detailed extraction procedures have been described in Hsu et al. (2007, 2010a).

Ionic species (Na^+, NH_4^+, K^+, Mg^{2+}, Ca^{2+}, F^-, Cl^-, SO_4^{2-} and NO_3^-) in the leachate were analyzed through a Dionex model ICS-1100 (for anions) and ICS-900 (for cations) ion chromatograph equipped with a conductivity detector (ASRS-ULTRA). Trace elements in the digestion solutions, including Al, Fe, Na, Mg, K, Ca, Ba, Ti, Mn, Co, Ni, Cu, Zn, Mo, Cd, Sn, Sr, Sb, Pb, Tl, Se, Ge, Cs, Ga, V, Cr, As, Se, and Rb, were analyzed by inductively coupled plasma–mass spectrometry (ICP–MS). Quality assurance and control of the ICP–MS was guaranteed by the analysis of a certified reference standard, NIST SRM-1648 (urban particulates). The resulting recoveries fell within ±10 % of the certified values for most elements, except for Se, As, Cs, Sb, and Rb (±15 %) (Hsu et al., 2009, 2010a).

2.1.5 OC and EC measurements

A punch of $0.526\,\text{cm}^2$ from each quartz filter was heated stepwise by a thermal/optical carbon analyzer (DRI 2001, Atmoslytic, US) in a pure helium atmosphere

Title Page

Abstract | Introduction

Conclusions | References

Tables | Figures

◄ | ►

Back | Close

Full Screen / Esc

Printer-friendly Version

Interactive Discussion

at 140 °C (OC1), 280 °C (OC2), 480 °C (OC3), and 580 °C (OC4), and then in 2 % O_2/98 % He atmosphere at 580 °C (EC1), 740 °C (EC2), and 840 °C (EC3) to convert any particulate carbon on the filter to CO_2. After catalyzed by MnO_2, CO_2 was reduced to CH_4, which was then directly measured. Mass concentrations of OC and EC were obtained according to the IMPROVE protocol (Chow et al., 2007), OC = OC1 + OC2 + OC3 + OC4 + OP; EC = EC1 + EC2 + EC3-OP, where OP is the optical pyrolyzed OC. Detailed descriptions can be found in Zhang et al. (2012a).

2.2 Data analysis methods

2.2.1 Chemical mass closure

In this study, we constructed chemical mass closure (CMC) on a seasonal basis by considering mineral dust, SO_4^{2-}, NO_3^-, NH_4^+, EC, particulate organic matter (POM), chloride salt (instead of sea salt; reason given below), trace element oxide (TEO), and biomass burning-derived K^+. SO_4^{2-}, NO_3^-, and NH_4^+ can be regarded as the secondary inorganic aerosols.

The aluminosilicate (i.e. soil, dust, or mineral) component is often estimated through the following formula (Malm et al., 1994; Chow et al., 1994), which includes Si.

$$[Mineral] = 2.20\,Al + 2.49\,Si + 1.63\,Ca + 2.42\,Fe + 1.94\,Ti$$
$$[Mineral] = 1.89\,Al + 2.14\,Si + 1.40\,Ca + 1.43\,Fe$$

However, Si is volatilized as SiF_4 in the acid digestion of aerosol samples when using HF. Therefore, a few studies estimated Si from Al in the calculation of the mineral component (Hueglin et al., 2005). However, once Al is used in estimating Si concentrations, it generates relatively large uncertainty in the mineral component proportion as Si/Al mass ratios could largely vary in China's dust (Yan et al., 2012, and references therein). Accordingly, we adopted a straightforward method conventionally used

in estimating dust aerosols from Al:

[Mineral] = Al/0.07

where 0.07 is the average Al content (7 %) reported by Zhang et al. (2003b). A similar
estimation has been applied previously (Ho et al., 2006; Hsu et al., 2010b).

In estimating POM, we adopted a factor of 1.6 in converting OC to POM (Viidanoja
et al., 2002), whereas a wide range of 1.4–2.2 has been utilized in previous investiga-
tions (Turpin and Lim, 2001; Andreae et al., 2008). The main determinants in selecting
a conversion factor are the origin and age of the organic aerosols. The factor of 1.6
was employed in this study because the latest result shows a OM/OC ratio averaged at
1.59 ± 0.18 in $PM_{2.5}$ over China (Xing et al., 2013). This factor was used for the $PM_{2.5}$
of Beijing by Dan et al. (2004), who also observed a similar seasonality for EC and OC
and a OC/EC ratio (2–3) close to our results.

Sea salt is usually calculated as [Sea salt] = $1.82 \times Cl^-$ or = $2.54\,Na^+$. Given that Bei-
jing is about 150 km away from East China's coastal oceans (i.e. Bohai Sea), sea spray-
generated sea salt particles are not readily transported and are therefore insignificant
to fine aerosols in Beijing. Nevertheless, dust blowing from Northern and Northwestern
China is often associated with NaCl and Na_2SO_4 from salt lake sediments and saline
soils (Zhang et al., 2009). On the other hand, Cl may be essentially contributed by
coal combustion in Beijing, particularly in winter (Yao et al., 2002). Thus, we consid-
ered chloride salt, instead of sea salt, as an individual component of $PM_{2.5}$ aerosols
in Beijing: [Cl salt] = $[Cl^-] + [Na^+] + [ss\text{-}Mg^{2+}]$. By considering chloride depletion in sea
salt particles within the marine boundary layer because of the heterogeneous reaction,
Hsu et al. (2010a) successfully evaluated such formula.

Following Landis et al. (2001), we estimated the contribution of heavy metals as
metal oxides by employing the following equation:

$$TEO = 1.3 \cdot [0.5 \cdot (Sr + Ba + Mn + Co + Rb + Ni + V) + 1.0$$
$$\cdot (Cu + Zn + Mo + Cd + Sn + Sb + Tl + Pb + As + Se + Ge + Cs + Ga)].$$

The enrichment factor (EF) of a given element (E) was calculated by using the formula $EF = (E/Al)_{Aerosol}/(E/Al)_{Crust}$ (Hsu et al., 2010a), where $(E/Al)_{Aerosol}$ is the ratio of the element to the Al mass in aerosols and $(E/Al)_{Crust}$ is the ratio in the average crust (Taylor, 1964). The result of the EF is shown in Fig. S1. Elements with EFs of ≤ 1.0, such as Cr and Y, were not considered, as they are of exclusive crustal origin. Elements with EFs between 1 and 5 were multiplied by a factor of 0.5, as they are possibly originated from two sources (i.e. anthropogenic and crustal sources). Elements with EFs ≥ 5.0 were multiplied by unity, as they are dominated by anthropogenic origins. Furthermore, the multiplicative factor was set at 1.3 so that metal abundance could be converted to oxide abundance, similar to those used by Landis et al. (2001). We also considered biomass burning-derived K^+ (K_{BB}) as an individual component, although K_{BB} salt may exist in the chemical forms of KCl and K_2SO_4 (Pósfai et al., 2004), where both Cl^- and SO_4^{2-} have already been considered in other components.

2.2.2 PMF model

PMF is an effective source apportionment receptor model that does not require the source profiles prior to analysis and has no limitation on source numbers (Hopke, 2003; Shen et al., 2010). The principles of PMF can be found elsewhere in detail (Han et al., 2006; Song et al., 2006, Yu et al., 2013). In the present study, PMF 3.0 was employed with the inclusion of 34 chemical species in the model computation: $PM_{2.5}$, Al, Fe, Na, Mg, K, Ca, Ba, Ti, Mn, Co, Ni, Cu, Zn, Mo, Cd, Sn, Sb, Pb, V, Cr, As, Se, Rb, Na^+, NH_4^+, K^+, Mg^{2+}, Ca^{2+}, Cl^-, SO_4^{2-}, NO_3^-, OC, and EC. Six physically realistic sources were identified.

2.2.3 Air mass back trajectory cluster

We calculated 48 h air mass back trajectories arriving at the sampling site (116.30° E, 39.99° N) during our sampling period by using the National Oceanic and Atmospheric Administration (NOAA) HYSPLIT-4 model with a 1° × 1° latitude–longitude grid and the

Chemical characterization and source apportionment

R. Zhang et al.

final meteorological database. The six hourly final archive data were generated from the National Center for Environmental Prediction's Global Data Assimilation System (GDAS) wind field reanalysis. GDAS uses a spectral medium range forecast model. More details about the HYSPLIT model can be found at http://www.arl.noaa.gov/ready/open/hysplit4.html (NOAA Air Resources Laboratory). The model was run four times per day at starting times of 04:00, 10:00, 16:00, and 22:00 UTC (12:00, 18:00, 00:00, and 06:00 LT, respectively). The arrival level was set at 100 m above ground level. The method used in trajectory clustering was based on the GIS-based software TrajStat (http://www.meteothinker.com/TrajStatProduct.aspx).

2.2.4 Potential source contribution function

The potential source contribution function (PSCF) is a method for identifying regional sources based on the HYSPLIT model. The zone of concern is divided into $i \times j$ small equal grid cells. The PSCF value in the ijth cell is defined as m_{ij}/n_{ij}, where n_{ij} is designated as the numbers of endpoints that fall in the ijth cell and m_{ij} denotes the numbers of "polluted" trajectory endpoints in the ijth cell. In this analysis, average concentrations were treated as the "polluted" standard (Hsu et al., 2003). To better reflect the uncertainty in cells with small n_{ij} values (Polissar et al., 1999), the weighting function w_{ij} was adopted:

$$w_{ij} = \begin{cases} 1.00 & 80 < n_{ij} \\ 0.70 & 20 < n_{ij} \leq 80 \\ 0.42 & 10 < n_{ij} \leq 20 \\ 0.05 & n_{ij} \leq 10 \end{cases}$$

The study domain was in the range of 75°–130° E, 30°–60° N. The resolution was 0.5° × 0.5°.

3 Results

3.1 Annual average

Table 1 provides a statistical summary of the obtained data on atmospheric concentrations for $PM_{2.5}$, Al (a tracer of aluminosilicate dust), water-soluble ions, OC, and EC during the sampling period. The annual mean $PM_{2.5}$ concentration reached $135 \pm 63 \, \mu g m^{-3}$. This mean value is nearly three times higher than that ($35 \, \mu g m^{-3}$) of the interim target-1 standard for annual mean $PM_{2.5}$ recommended by the WHO. The level of $PM_{2.5}$ in Beijing is much higher than other megacities around the world. In comparison with that of domestic cities, $PM_{2.5}$ seems to display a spatial tendency, increasing northward and decreasing southward (Zhang et al., 2012b). Such a spatial pattern may be related to the low rainfall and high dust in northern China (Qian et al., 2002, 2005). According to Wang et al. (2008), $PM_{2.5}$ concentrations in winter were much higher than in summer in 2001 to 2002. However, such a trend seemed to be reversed in 2005 to 2006, with rather higher concentrations in summer.

For the ionic concentrations, SO_4^{2-} ranked the highest among the water-soluble ions analyzed, with an annual mean of $13.6 \pm 12.4 \, \mu g m^{-3}$, followed by NO_3^- ($11.3 \pm 10.8 \, \mu g m^{-3}$), NH_4^+ ($6.9 \pm 7.1 \, \mu g m^{-3}$), Ca^{2+} ($1.6 \pm 1.4 \, \mu g m^{-3}$), Cl^- ($1.4 \pm 2.2 \, \mu g m^{-3}$), K^+ ($0.92 \pm 0.75 \, \mu g m^{-3}$), Na^+ ($0.46 \pm 0.55 \, \mu g m^{-3}$), and Mg^{2+} ($0.16 \pm 0.13 \, \mu g m^{-3}$). Such levels of mean concentrations are rather comparable with those measured in many Chinese cities such as Shanghai, Tianjin, Jinan, and Guangzhou (Yao et al., 2002; Tao et al., 2009; Gao et al., 2011; Gu et al., 2011). On average, the combination of SO_4^{2-}, NO_3^-, and NH_4^+, which could be regarded as secondary inorganic aerosols, constituted the majority (88 %) of the total ionic concentrations, consistent with earlier studies (Yao et al., 2002; Duan et al., 2003). The annual mean concentrations of OC and EC reached up to 17.0 ± 10.0 and $5.0 \pm 4.4 \, \mu g m^{-3}$, respectively. Such levels are close to those observed for regional sites across China ($16.1 \pm 5.2 \, \mu g m^{-3}$ for OC and $3.6 \pm 0.93 \, \mu g m^{-3}$ for EC) by Zhang et al. (2008), who extensively measured

carbonaceous aerosols around China; however, such concentrations are approximately half of those observed at urban sites ($33.1 \pm 9.6\,\mu g\,m^{-3}$ for OC and $11.2 \pm 2.0\,\mu g\,m^{-3}$ for EC) by Zhang et al. (2008).

3.2 Seasonality

As illustrated in Fig. 2, the seasonalities of $PM_{2.5}$ and these primary species were characterized by distinctive features. The seasonality of $PM_{2.5}$ concentration was not very evident and typical, with nearly equal concentrations of around $140\,\mu g\,m^{-3}$ in summer, autumn, and winter and a relative minimum ($\sim 125\,\mu g\,m^{-3}$) in spring. The minimum concentration typically occurs in summer because precipitation in Beijing is usually concentrated at that period. However, this is not the case, because the maximum concentrations of secondary sulfate and ammonium were observed in summer, arising from strong photochemistry and accounting for a large proportion ($\sim 25\,\%$) of $PM_{2.5}$ in Beijing (Yao et al., 2003).

In contrast to $PM_{2.5}$, sulfate and ammonium revealed a typical seasonality with higher concentrations in spring and summer and lower concentrations in autumn and winter, consistent with the seasonal variability of AOT (Xia et al., 2006). The summertime maximum concentrations of sulfate and ammonium were 24 and $12\,\mu g\,m^{-3}$, respectively, which were higher than those in Beijing before 2003 (~ 15 and $\leq 10\,\mu g\,m^{-3}$, respectively) (He et al., 2001; Duan et al., 2006; Wang et al., 2005) but rather comparable to those observed in the last few years (Okuda et al., 2011; Song et al., 2012). By contrast, the wintertime concentration of sulfate ($8.5\,\mu g\,m^{-3}$) was significantly reduced compared with earlier literature data (He et al., 2001; Hu et al., 2002; Wang et al., 2005). The decrease in wintertime sulfate concentration seemed to result from the effective control of SO_2 emissions from coal combustion (Hao et al., 2005). High summertime sulfate concentration is ascribed to enhanced photochemistry during summer, and relatively high humidity accelerates the conversion rate of SO_2 to the particulate form (Yao et al., 2003). However, the precursor SO_2 concentrations are much higher in winter (Fig. S2) because of domestic heating (Hu et al., 2002b). In the present study,

artificial biases, particularly of nitrate and ammonium, possibly occurred during sampling because no denuder and/or back-up filter was used to trap ammonia and nitric acid (Pathak et al., 2004). The maximum concentration ($15.5\,\mu g\,m^{-3}$) of nitrate was observed in spring rather than summer, which was different from that of sulfate (Wang et al., 2008). This observation may be ascribed to the volatility of ammonium nitrate, which is one of the main chemical forms of nitrate associations revealed by the ionic relationships. Thus, ammonium nitrate could evaporate at relatively high temperature. Besides, there are distinct emission sources for their respective precursor gases, SO_2 and NO_x. The minimum concentration of nitrate was observed in winter. Nitrate levels could be a function of various factors in terms of emissions, such as exhaust, coal combustion, and biomass burning, and complex chemical processes with respect to photochemistry, heterogeneous reaction, renoxification, and gas–aerosol equilibrium. Rapid increases in on-road vehicular numbers in Beijing may offset any control measures for NO_x emissions, especially from coal combustion.

Crustally derived ions and elements, such as Mg^{2+}, Ca^{2+}, and Al, waxed in the spring and waned in the summer, followed by significant increases toward autumn and winter. Such levels of seasonal mean concentrations and seasonalities are consistent with those observed in previous studies (Duan et al., 2006; Wang et al., 2005), which are related to dust storms and anthropogenic and fugitive dust. The seasonal concentrations of Na^+ and Cl^- peaked in winter, consistent with Hu et al. (2002) and Wang et al. (2005). The seasonality of Mg^{2+} was distinguishable from that of Na^+, demonstrating the difference in their dominant sources. K^+ had relatively higher concentrations in both spring and autumn than in summer and winter, which was closely associated with the agricultural burning around Beijing (Zheng et al., 2005). Such seasonality was distinct from those of previous studies, in which winter often had the highest concentration (He et al., 2001; Duan et al., 2006; Wang et al., 2005).

Both OC and EC had similar seasonal patterns of waxing in winter and waning in spring (for EC) or summer (for OC). Zhang et al. (2008) observed a persistently common seasonality for both OC and EC at 18 background, regional, and urban stations

Title Page

Abstract | Introduction

Conclusions | References

Tables | Figures

|◀ | ▶|

◀ | ▶

Back | Close

Full Screen / Esc

Printer-friendly Version

Interactive Discussion

in China, namely, a maximum in winter and a minimum in summer. The seasonalities may be governed by the variability in emission strengths and meteorology. For instance, lower-molecular weight semi-volatile organic compounds are mostly in gaseous phase at high temperature in summer (Yassaa et al., 2001). The OC/EC mass ratio 2.0 indi-

5 cates the presence of secondary organic matter (Chow et al., 1996). In this work, the OC/EC ratios mostly fell within the range of 2–5, with mean ratios of 4.8, 2.5, 3.0, and 2.7 in spring, summer, autumn, and winter, respectively (Fig. 3). These figures are very similar to those observed in previous studies (Duan et al., 2006; Zhang et al., 2008), which suggests the relative domination of secondary organic aerosols in spring but of

10 primary sources in other seasons (Zhang et al., 2008). Another reason for the relatively higher springtime OC/EC mass ratio may be the open biomass burning source, consistent with higher K^+ in the spring (Fig. 2), as the aerosols from open biomass burning are generally characterized by elevated OC/EC ratios (Cao et al., 2007).

3.3 Stoichiometric analyses of cations and anions

15 Note that equivalent concentrations ($\mu eq\, m^{-3}$) are used throughout this section. Figure 4 shows the scatter plots of (a) Mg^{2+} vs. Na^+, (b) Mg^{2+} vs. Ca^{2+}, (c) Cl^- vs. Na^+, and (d) Cl^- vs. K^+. Figure 5 shows the scatter plots of (a) total cations vs. total anions, (b) NH_4^+ vs. SO_4^{2-}, (c) NH_4^+ vs. $[SO_4^{2-} + NO_3^-]$, (d) $[NH_4^+ + Ca^{2+}]$ vs. $[SO_4^{2-} + NO_3^-]$, (e) $[NH_4^+ + Ca^{2+} + Mg^{2+}]$ vs. $[SO_4^{2-} + NO_3^-]$, and (f) $[NH_4^+ + Ca^{2+} + Mg^{2+}]$

20 vs. $[SO_4^{2-} + NO_3^- + Ex\text{-}Cl^-]$. Ex-$Cl^-$ is the excessive Cl^-, defined as the excessive amount of Cl^- relative to the amount sea salt can sustain with Na^+ as the tracer of sea salt: Ex-$Cl^- = Cl^- - [Na^+] \cdot 1.17$, where 1.17 is the typical Cl/Na^+ equivalent ratio of average seawater (Chester, 1990). If the resulting Ex-Cl^- is negative, then no Cl^- excess exists. In other words, Cl^- is totally contributed by sea salt and is even depleted

25 by heterogeneous reactions. Nevertheless, total Na^+ does not necessarily originate from sea salt alone, but could partially come from dust. The resultant biases are hence likely insignificant.

Figure 4a illustrates that Mg^{2+} mostly comes from non-sea salt sources, except in wintertime, because the regression slopes that represent the Mg^{2+}/Na^+ ratios (1.56, 0.70, 0.68, and 0.25 for spring, summer, autumn, and winter, respectively) are clearly deviated from the ratio (0.23) of average seawater (Chester, 1990). Instead, the domi-

5 nant source of Mg^{2+} is mineral dust, mainly carbonate minerals (Li et al., 2007), as reflected by the good correlations (0.97, 0.83, 0.90, and 0.80 for spring, summer, autumn, and winter, respectively) between Mg^{2+} and Ca^{2+} (Fig. 4b). Similarly, most Cl^-/Na^+ ratios (1.70, 1.21, 2.51, and 2.25 for spring, summer, autumn, and winter, respectively) in $PM_{2.5}$ are larger than the mean ratio (1.17) of seawater, except the summertime sam-

10 ples (Fig. 4c). This difference indicates the dominance of the non-sea salt sources, of which the most likely contributor of Cl^- is coal combustion (Yao et al., 2002), particularly in winter when Cl^- and SO_2 are maximal (Figs. 2 and S2). In summer, air masses are dominated by the southerly monsoon from Bohai (as supported by the trajectories below), leading to a mean Cl^-/Na^+ ratio close to that of average seawater. Moreover,

15 the correlations between K^+ and Cl^- largely varied with the seasons, with better correlation and higher ratios in autumn and winter and moderate correlations and lower ratios (less than unity) in summer and spring (Fig. 4d). Thus, the results suggested that K^+ was not present in chemical form KCl at high temperature, but as K_2SO_4 (Pósfai et al., 2004). By contrast, low temperature in winter may favor the presence of KCl.

20 Furthermore, the ratio of total cation concentration to total anion concentration is averaged at near unity throughout the year (Fig. 5a), which indicates excellent charge balance in $PM_{2.5}$ and high data quality. Figure 5b shows good correlations between NH_4^+ and SO_4^{2-} for the annual data set, with ratios (represented by the slope of the linear regression line) between 1.25 and 1.77 (all higher than unity). These good correlations

25 reveal the dominance of $(NH_4)_2SO_4$ (Ianniello et al., 2011), rather than NH_4HSO_4 and the possible full neutralization of SO_4^{2} by NH_4^+ throughout the year. We further considered the combination of NO_3^- and SO_4^{2-} in this charge balance analysis (Fig. 5c). The resulting NH_4^+ to $[SO_4^{2-} + NO_3^-]$ ratios ranged from 0.83 to 0.94 (all lower than unity),

which demonstrates the presence of NH_4NO_3 in the fine mode aerosols. Moreover, ratios lower than unity suggest that nitrate may be present in other chemical forms than NH_4NO_3. Heterogeneous reactions between NO_x (and its products, such as HNO_3 and N_2O_5) and dust carbonate are often observed in northern China (Li and Shao, 2009).

5 Accordingly, we examined the correlations of $[NH_4^+ + Ca^{2+}]$ vs. $[SO_4^{2-} + NO_3^-]$ (Fig. 5d) and of $[NH_4^+ + Ca^{2+} + Mg^{2+}]$ vs. $[SO_4^{2-} + NO_3^-]$ (Fig. 5e), given that the good correlations between Mg^{2+} and Ca^{2+} suggest the possible existence of water-soluble Mg in reacted carbonate dust. These ions are strongly correlated throughout the year, with high coefficients (all 0.99 or higher) and slopes of regression lines around unity. These

10 correlations indicate that nitrate is partly present in $Ca(NO_3)_2$ and $Mg(NO_3)_2$, not just in NH_4NO_3. We assumed that fine sized sulfate is exclusively associated with ammonium and that Na^+ is present only in the associated NaCl. However, these assumptions may not always be true because Na_2SO_4 is observed in dust particles from dried lakes in northern China (Zhang et al., 2009a) and NaCl could react with nitric acid to form

15 $NaNO_3$ via heterogeneous reaction (Hsu et al., 2007). Therefore, based on the aforementioned equivalent interrelationships and assumptions, we quantitatively estimated that the former two chemical forms ($Ca(NO_3)_2$ and $Mg(NO_3)_2$) represent ~ 20 % of the total nitrate and that NH_4NO_3 is the dominant association accounting for the remaining ~ 80 %. The elevated Cl^-/Na^+ ratio (> 1.17) shows that excessive Cl^- seemed to be

20 attributed to coal combustion rather than sea salt particles from dried salt lake sediment. The addition of excessive Cl^- (Fig. 5f) insignificantly changed the correlations of positive and negative charges. Nevertheless, we noted that in wintertime, the equivalent ratio improved from 1.10 to 1.00, which indicates the presence of chloride salts such as KCl, $CaCl_2$, and $MgCl_2$ other than NaCl at low ambient temperature (Ianniello

25 et al., 2011). KCl may have originated from biomass burning, and $CaCl_2$ and $MgCl_2$ could have been formed through heterogeneous reactions between the dust carbonate and HCl emitted from coal combustion.

3.4 Chemical mass closure

By employing the methods in Sect. 2.2.1, we constructed the CMC of $PM_{2.5}$ in Beijing on a seasonal and annual basis. The reconstructed $PM_{2.5}$ mass concentrations were compared with the gravimetric $PM_{2.5}$ mass concentrations, as shown in Fig. 6, which shows a good correlation with one another in each season and throughout the year. However, the ratios seasonally changed, with higher ratios of 0.82 in spring and 0.75 in winter and lower ratios of 0.59 in summer and 0.68 in autumn. The proportions of all specific components in $PM_{2.5}$ together with the unidentified constituents as a whole are schematically illustrated by five pie charts for the four seasonal and annual cases (Fig. 7). Overall, the major components are secondary inorganic aerosols (combination of sulfate, nitrate, and ammonium), mineral dust, and POM, which account for each $\sim 20\%$, albeit with seasonal variations. The minor components include EC, chloride salt, potassium salt, and TEO, each of which represents less than 5%. Specifically, the proportions of mineral dust are maximal (33.4%) in spring, minimal (only 8.2%) in summer, and intermediate (23.6 and 28.9%) in the other two seasons, consistent with the tendency of seasonal Al concentrations. The totals of secondary inorganic species (SO_4^{2-}, NO_3^-, and NH_4^+) have the largest proportion (27% to 30%) in spring and summer and a minimal percentage ($< 15\%$) in autumn and winter. However, sulfate peaks were noted in summer (15.4%), whereas nitrate peaks were observed in spring (11.1%). Ammonium decreased from around 5 to 7% in spring and summer to half (2 to 3%) in autumn and winter. The POM fractions largely varied as follows: summer (14.7%) < spring (18.9%) < autumn (22.1%) < winter (28.6%). EC and chloride salt exhibited the largest proportions (5.2 and 3.3%, respectively) in winter. Potassium salt and TEO had slightly higher proportions in spring and autumn than in summer and winter.

Both the primary and secondary components of $PM_{2.5}$ in Beijing are equally important, albeit with seasonal variability, which is typical of PM pollution in China (Shao et al., 2006). In general, given that the seasonal variability in $PM_{2.5}$ mass

concentrations is relatively small, temporal trends in the proportions of each component of $PM_{2.5}$ resemble the atmospheric concentrations of their corresponding chemical species. The likely factors for such seasonalities are partially addressed in Sect. 3.2 and discussed in detail in the following two sections.

On average, the unidentified components reached 28.6 % of the total $PM_{2.5}$. They also showed seasonal variability, with the smallest (15.9 %) in spring when dust was prevalent, and the largest (42.5 %) in summer when secondary inorganic aerosol formation was favorable. Such high uncertainties in the CMCs were caused by the water absorption of water-soluble components in the weighing environment, though relative humidity was controlled (Speer et al., 1997; Tsai and Kuo, 2005). The absorption likely led to positive biases in $PM_{2.5}$ concentrations. Alternatively, such uncertainties may be partly due to the volatilization of NH_4NO_3 and organic matter, particularly in summer and autumn during the storage of the weighted samples prior to extraction, which may have resulted in negative biases in the specific components. Another likely reason for the non-match of the reconstructed and gravimetric mass concentrations is the varying factors used in transferring a given analyzed species (e.g. OC and Al) to a certain component (e.g. POM and mineral soils) (Rees et al., 2004; Hsu et al., 2010a; Yan et al., 2012). For example, a few studies adopted a factor of only 1.4 for converting OC content to organic matter (Duan et al., 2006; Song et al., 2007; Guinot et al., 2007). Another study obtained a much higher POM/OC mean ratio over China (Xing et al., 2013) of up to 1.92 ± 0.39 based on a mass balance method. If we adopt this higher ratio, the unidentified percentage would be reduced by 3 %. In the present study, the EF_{crust} of Ca averages at 2.6, which shows its enrichment relative to average crust composition. In Beijing, fine sized Ca-rich dust is partly attributed to construction activities. Therefore, we may underestimate carbonate abundance in the mineral component estimated from Al concentration alone (Guinot et al., 2007). This may have resulted in the underestimation (~ 2 %) of the total mass reconstructed.

4 Discussion

4.1 Source identification and apportionment

By utilizing the PMF model with the obtained full data set as input data, we identified six main sources: mineral dust, biomass burning, coal combustion, traffic emissions plus waste incineration, industrial pollution, and secondary inorganic aerosol. These sources have average contributions of 15, 18, 12, 4, 25, and 26 %, respectively (Table 2). Figures 8 and 9 show the modeled source profiles and the time series of modeled concentrations for each identified main source, respectively. Table 2 summarizes the source apportionment results of the relative contributions from each identified source to the $PM_{2.5}$ on both seasonal and annual bases in Beijing. Again, the relative dominance of each identified source largely varies with changing seasons, which is roughly consistent with the CMC results. For mineral dust, only one of the six sources mostly dominated by nonvolatile substance, its proportions (e.g. annual mean ~ 20 %) and relative order in the four seasons are consistent with the CMC results, with higher contribution in spring, lower contribution in summer, and intermediate contribution in autumn and winter. This consistency indirectly verifies the reliability of the PMF results. The other five sources all appear to be related to high-temperature activities and/or photochemical processes and involved with volatile species. We then compared the contribution percentages of the secondary inorganic aerosol (SIA) with the CMC results as this source is also identified in the CMC analyses. Apparently, the percentages of SIA in the four seasons differ from those obtained by CMC in terms of the values (e.g. 6 to 54 % versus 14 to 33 % for SIA), although the seasonal trends are quite similar. Thus, CMC method only offers chemical characterization instead of source apportionment. The PMF model provides real information on sources of aerosol speciation.

Moreover, we evaluated the distinctive characteristics of each modeled source profile according to well-accepted knowledge. The first component, mineral dust, is typically characterized by high crustal elements, such as Al, Ca (Ca^{2+}), Fe, Mg, K, and Ti. Ca content is higher than Al, which indicates Ca-rich dust. OC content is close

to ~ 12 %, which suggests resuspended dust because of the presence of high levels of OC (Watson and Chow, 2001). Thus, this source possibly mixes desert/loess dust, anthropogenic construction dust, fugitive dust, and resuspended road dust. Construction activities are prevalent in the urban cities of China, and no effective measures for dust control are implemented. Therefore, calcium is used as an indicator element for construction dust in Beijing (Zhang and Iwasaka, 1999). The second source, coal combustion, is characterized by elevated Cl^- associated with high Na^+, OC, and EC. Extraordinarily high Cl^- associated with fine aerosols in winter is a distinctive feature in Beijing and even around inland China, which is ascribed to coal combustion (Yao et al., 2002; Wang et al., 2008). Coal combustion in China is the predominant source of fine aerosols over China (Yao et al., 2009), especially of mercury in the atmosphere, not only in the Northern Hemisphere but also around the globe (Pirrone et al., 2010). Coal fly ash contains abundant Pb because of ineffective dust removal in power plants and residential boilers (Zhang et al., 2009b). Sodium is enriched in fine particulates from coal combustion (Takuwa et al., 2006). Wang et al. (2008) and Zhang et al. (2009a) attributed such high Na and Cl to the presence of Na_2SO_4 and NaCl that may have originated from dried lake salt sediment in Inner Mongolia, a non-local dust source. However, as discussed, salt lake aerosols alone cannot account for such strikingly high Cl^- in winter, which suggests that coal combustion is the most likely dominant source. Different investigations have obtained significantly different contributions of coal combustion to $PM_{2.5}$ in Beijing, which range from 7 to 19 %. Yao et al. (2009) concluded that the likely fraction ranges between 15 and 20 %. Nevertheless, previous studies have not considered that other main identified sources, such as secondary inorganic and organic aerosols, have contributions from coal combustion.

The third source, biomass burning, is characterized by high K (K^+), which is an excellent tracer of biomass burning aerosols (Cachier and Ducret, 1991; Watson and Chow, 1998), and by rich Rb, OC, and NO_3^-. Biomass burning has higher contributions in spring and autumn than in summer and winter, consistent with cultivation in spring and harvest in autumn. The fourth source is a mixed source of traffic and metropolitan

incineration emissions, which is characterized by high NO_3^-, EC, Cu, Zn, Cd, Pb, Mo, Sb, and Sn. These aerosol species are all enriched in vehicular and/or waste incineration emissions (Lee et al., 1999; Alastuey et al., 2006; Birmili et al., 2006; Marani et al., 2003; Dall'Osto et al., 2012; Tian et al., 2012). For instance, Wåhlin et al. (2006) observed that traffic-generated aerosol particles are rich in Cu, Zn, Mo, and Sb. Christian et al. (2010) analyzed the aerosol particles emitted from garbage burning, which are rich in Zn, Cd, Sb, and Sn. Leaded gasoline was phased out in 1997 in Beijing and in 2000 in the rest of China. Coal burning was then suggested as the most important source of Pb aerosols in China (Mukai et al., 2001). However, Widory et al. (2010) argued that in Beijing, metal refining plants are the dominant sources of aerosol Pb, followed by thermal power stations and other coal combustion sources.

The fifth source is industrial pollution, which is characterized by high contents of OC, EC, Zn, Mn, and Cr. This source may also be involved with secondary organic aerosols. Coal is the primary energy source commonly used in industries in China. Both coal combustion and vehicle emissions are the main sources of primary OC (Zhang et al., 2007; Cao et al., 2011). However, Zhang et al. (2008) estimated that secondary OC represents more than half of the measured OC at regional sites ($\sim 67\%$) and urban sites ($\sim 57\%$), which is higher than those reported by Cao et al. (2007) (i.e. 30 to 53 %). Therefore, industrial pollution could act as a vital source of carbonaceous aerosols, which seems to be widely ignored. Furthermore, given that Zn and Cr contents are high, this source may be relevant to smelters and metallurgical industries (Dall'Osto et al., 2012). The sixth source is relevant to secondary inorganic aerosols, which are typically characterized by remarkable SO_4^{2-}, NO_3^-, and NH_4^+. Certain identified sources, such as biomass burning, coal combustion, vehicle exhausts, and waste incineration, can also contribute to secondary inorganic and organic aerosols through the emission of their precursor gases.

Figure 9 illustrates the time series of daily concentrations contributed by each identified source. To examine if the results are reasonable, we compared the modeled seasonalities of each source with the observed seasonalities of the specific chemical

species that could represent respective contribution sources (Fig. 2). For instance, we compared the maximal and minimal contributions of mineral dust in spring and summer, respectively, which are consistent with the seasonality of aerosol Al. Dust storms are essentially responsible for springtime dust aerosols, whereas in autumn and winter,

5 fugitive dust from construction and the resuspension of street dust are the main contributors. Obviously, the reconstructed time series of daily concentrations from coal combustion reveals a pronounced wintertime maximum, consistent with those of aerosol Cl^- (Fig. 2) and even gaseous SO_2 (Fig. S2). Moreover, the time series of biomass burning contributions show relatively higher concentrations in spring and autumn and

10 lower concentrations in summer and winter, consistent with the seasonality of K^+. For traffic and waste burning emissions, the resulting time series do not reveal evident seasonality, corresponding with the seasonalities of nitrate and some trace metals, such as Pb, Cu, Sb, and Cd (Fig. S3). Industrial pollution has higher contributions in summer and autumn, possibly corresponding with the seasonalities of Zn and Cr. However, such

15 seasonality is inconsistent with that of OC, with a wintertime maximum, because OC may be from various sources, including the former five sources identified. Coal combustion has the largest contribution in winter, and low temperature in winter facilitates the formation of secondary organic aerosols. SIA has higher contributions in summer and spring, mirroring the seasonalities of sulfate, nitrate, and ammonium. This result

20 is definitely related to the photochemistry that accounts for SIA formation. The formed SIA species may not appear in their original emission sources (i.e. coal combustion, biomass burning, traffic exhausts, waste incineration, and industrial pollution), but in the SIA component. Based on the PMF results based and chemical data in January and August 2004, Song et al. (2007) found that the most predominant sources of $PM_{2.5}$ are

25 coal combustion in winter and secondary aerosols in summer, along with other significant sources, such as motor vehicle emissions, road dust, and biomass burning. The PMF-modeled results seem to be promising because the corresponding time series of each source's contribution are very consistent with the observations.

4.2 Regional sources deduced from trajectory and PSCF analyses

The regional sources and transport of air pollutants exert a profound impact on local air quality in Beijing (e.g. Wang et al., 2004). To address this issue, both trajectory clustering and PSCF methods were employed. The 48 h back trajectories start-
5 ing at 100 m from Beijing were computed by using the HYSPLIT model of NOAA (http://www.arl.noaa.gov/ready.html). Four clusters were made (Fig. 10): northwestern (including western, NW), northern (N), eastern (from northeastern to southeastern, E), and southern (S) directions. The NW cluster was further differentiated into two types, namely, fast (NW_f) and slow (NW_s), according to the motion speed ($\leq 7\,m\,sec^{-1}$ for
10 NW_s and $> 7\,m\,sec^{-1}$ for NW_f,) and distance of air parcels. The classification is consistent with the spatial distribution of fine AOD retrieved by remote sensing (Fig. 1).

Table 3 summarizes the percentages of each trajectory cluster in the total on annual and seasonal bases and the corresponding mean concentrations of $PM_{2.5}$ and various aerosol species associated within each trajectory cluster. Annually, the trajectory clus-
15 ters are dominated by both NW and S, accounting for 44 % and 34 %, respectively. The E and N clusters represent the rest (15 % and 7 %, respectively). However, the variability is large and season-dependent. For instance, the predominant clusters are N (30 %) and S (44 %) in spring, S (73 %) in summer, NW_f (50 %) in autumn, and NW_f (88 %) in winter. The resulting mean concentrations of main aerosol species seasonally vary
20 with certain types of air masses. In winter, a few $PM_{2.5}$ pollution cases (only 12 % of the wintertime trajectories) with mean concentration as high as $209\,\mu g\,m^{-3}$ are associated within the E trajectories that passed over Hebei and Liaoning Provinces, where heavy industries are concentrated in certain cities (e.g. Tianjin, Tangshan, Dalian, Shenyang). However, in spring, summer, and autumn, high $PM_{2.5}$ ($> 150\,\mu g\,m^{-3}$) is preferentially
25 associated with the S trajectory cluster. Overall, the general patterns agree with the spatial distribution of the MODIS retrieved fine AOD around Beijing (Fig. 1).

Furthermore, we applied an alternative approach called PSCF to explore the likely regional sources and transport pathways of various $PM_{2.5}$ associated speciations, such

as sulfate, nitrate, ammonium, OC, EC, and mineral dust in Beijing, as illustrated in Fig. 11. A few main features were found: (a) sulfate, nitrate, and ammonium have similar spatial patterns, with higher values in the east to the south, covering Tianjing, Shijiazhuang, and Zhengzhou; (b) both OC and EC show similar spatial distribution,
5 with higher values in the northwest, the south, and the northeast, covering the border of Hebei and Shanxi Provinces, Inner Mongolia, the border of the Hebei, Shanxi, and Henan Provinces, and the area from Tianjing to Shenyang; (c) the higher value for mineral aerosols is localized in the northwest and the south; and (d) for these six aerosol speciations, the southern area appears to be a common hot spot. The overall
10 PSCF results are rather consistent with the spatial distribution of fine AOD (Fig. 1). The statistics obtained from the trajectory clustering (Table 3) shows that the southern air masses bring high levels of secondary inorganic and carbonaceous aerosols and the northwestern air masses are enriched in mineral dust and carbonaceous aerosols. Sun et al. (2006) and Street et al. (2007) found that the S sector has much higher sec-
15 ondary species, such as sulfate, nitrate, and ammonium. During haze-fog events in Beijing, chemical constituents of secondary inorganic aerosols are also much higher when the winds blow from the south. Such high amounts of secondary fine-sized aerosols in southern air parcels may be related to high humidity (water vapor) and enhanced heterogeneous reaction in clouds/fog, aside from strong photochemistry. The associa-
20 tion of high dust with the NW trajectories is consistent with Wang et al. (2004) and Yu et al. (2011).

4.3 Implications for atmospheric chemistry, PM control measures, and climate

Rigorous efforts exerted for air pollutant governance prior to the 2008 Beijing Summer Olympics, such as changing the energy source structure, reducing local dust emis-
25 sions, controlling vehicle exhaust emissions, and relocating major industrial emitters, have achieved air quality improvement during the games. Effective control of coarse PM pollution seemed possible and the main urban air pollutants became finer PM ($PM_{2.5}$). The annual mean concentration of $PM_{2.5}$ in Beijing is nearly three times and

over an order of magnitude higher than the annual exposure level ($35\,\mu g\,m^{-3}$) and air quality guideline (only $10\,\mu g\,m^{-3}$) recommended by the WHO, which indicates that tremendous efforts of multi-pollutant alleviation measures and air quality management policies are still needed for PM abatement (Zhang et al., 2012b). The PM pollution

5 level in Beijing is governed by the emission sources involved with natural and anthropogenic origins and particulate and gaseous phases and by synoptic meteorological conditions and atmospheric circulation systems. With sulfate/SO_2 as an example, our results demonstrate that meteorological conditions could be a crucial factor for determining fine aerosol levels and formation other than their own and/or precursor emission

10 strengths. Accordingly, this study offers insights into the likely impact on atmospheric chemistry because of the changing climate. The increasingly warm climate predicted (IPCC, 2007) will enhance photochemistry in summer, which may offset the mitigation measures in China to some extent. Moreover, the decreasing wind speed forecasted in China (Chen et al., 2012) favors air quality degradation because of the likely re-

15 duction in ventilation efficiency (Zhang et al., 2007; Song et al., 2008). Complex PM pollution in terms of chemical and physical properties such as multiple sources (natural versus anthropogenic), mixing states (internal versus external), various chemical composition, size spectrum, and hygroscopicity, which are closely related to optical and direct/indirect radiative properties, complicate the modeling assessment of aerosol ef-

20 fects on the climate (cooling versus warming) in China and in the region.

If the contributions from the three main sources (coal combustion, industrial pollution, and SIA) are combined, fossil fuel burning related emissions may dominate $PM_{2.5}$ pollution in Beijing, representing two thirds ($\sim 68\,\%$) of $PM_{2.5}$. Rapid industrial development in provinces around Beijing, including Liaoning, Hebei, Shandong, Shanxi, and

25 Henan, has exacerbated regional air quality because of massive quantities of air pollutant emissions, resulting in cross-border transport. Better understanding of the pollution characteristics of $PM_{2.5}$ in Beijing, particularly after the 2008 Summer Olympics, in terms of chemical composition and sources of $PM_{2.5}$ from a regional and seasonal perspective, is urgently needed. Relevant air pollution control measures should be

implemented locally, regionally, and nationally in China. Such measures would improve pollution abatement, public health, and climatic modeling capacity.

5 Summary

The levels of daily PM$_{2.5}$ concentrations are still elevated in Beijing throughout the year, with an annual mean of up to $135 \pm 63\,\mu g\,m^{-3}$, which is several times higher than the 24 h exposure standard and guideline recommended by the WHO. Seasonality is not very evident, although the highest occurred in winter and the lowest in spring. Distinctive seasonalities occurred for various aerosol species. Sulfate and ammonium peaked in summer, mainly because of photochemistry, whereas the maximum of nitrate was observed in spring, which is attributed to the heterogeneous reaction between dust carbonate and nitric acid (the product of NO$_x$) along with the photochemical process. Crustally derived species, such as Ca^{2+}, Mg^{2+}, and Al, showed typical seasonality, waxing in spring and waning in summer. The maximum of OC, BC, and Cl was observed in winter, and their minimum in summer or spring, which suggests a relation with fossil fuel (mainly coal) combustion processes. The correlations between total cation and anion equivalent concentrations were excellent with a mean ratio around unity, which indicates good charge balance. The mean NH$_4^+$/SO$_4^{2-}$ equivalent concentration ratios were higher than unity throughout the year, which reveals that NH$_4^+$ could fully neutralize sulfuric acid. The correlations between NH$_4^+$ and [SO$_4^{2-}$ + NO$_3^-$] suggest that ammonium could partially be present as NH$_4$NO$_3$. Furthermore, the correlations between [NH$_4^+$ + Ca^{2+}] and [SO$_4^{2-}$ + NO$_3^-$] demonstrate the presence of Ca(NO$_3$)$_2$ and NH$_4$NO$_3$, which was due to the heterogeneous reaction between dust carbonate and nitric acid. A few chloride salts may form, particularly in winter when low temperature is favorable for their occurrence.

CMCs were successfully constructed on a seasonal basis, although with an unidentified fraction averaged at 28.6 %. The major aerosol speciation considered in this study

Title Page

Abstract | Introduction

Conclusions | References

Tables | Figures

◄ | ►

◄ | ►

Back | Close

Full Screen / Esc

Printer-friendly Version

Interactive Discussion

included mineral dust, POM, and SIA (the combination of sulfate, nitrate, and ammonium), and the minor components were EC, chloride salts, trace element oxides, and biomass burning-derived potassium salts. Their respective fractions in $PM_{2.5}$ largely varied with the season, generally corresponding to the seasonalities of their concen-
5 trations. The higher unidentified fraction, particularly in summer, may be partly due to the volatilization of volatile or semi-volatile species, such as ammonium nitrate and organic species. This observation highlights the requirement for the immediate analysis of aerosol samples after collection. Through the PMF model, six potential sources were identified: mineral dust, coal combustion, biomass burning, traffic and waste incinera-
10 tion emission, industrial pollution, and SIA. Similarly, the relative contributions of these sources to $PM_{2.5}$ in Beijing greatly varied with the changing seasons, which proves the "Complex Air Pollution" in Beijing. On the average, the annual mean contributions were 15, 18, 12, 4, 25, and 26 %, respectively. The highest contributions occurred in spring for soil dust (23 %) and traffic and waste incineration emission (5 %), in winter for coal
15 combustion (57 %), in autumn for industrial pollution (42 %), in summer for SIA (54 %), and in both spring and autumn for biomass burning (19 and 17 %, respectively). Based on the trajectory clustering and PSCF method results, regional sources and transport pathways of various aerosol speciation associated with $PM_{2.5}$ in Beijing were explored. The southern region may be an important source of all major aerosol components. The
20 eastern region is significant for anthropogenic species such as SIA and carbonaceous aerosols. The northwestern region could be the common source of naturally derived mineral dust and anthropogenically derived carbonaceous aerosols. This observation indicates that air pollution control measures must be simultaneously implemented in the surrounding provinces.
25 The results of our studies clearly suggest that chemical constituents and sources of $PM_{2.5}$ can largely vary with seasons, which are characterized by variable meteorology and diverse air pollution sources. Source apportionment results do not precisely reflect the large temporal contribution variations from various sources when PMF analyses using data from the full four seasons are not considered. In addition, apart from the

emission strengths of primary aerosols and gaseous precursors, the dynamically variable synoptic weather conditions and circulation patterns also have a crucial role in governing the anomalies of PM (both fine and coarse size) concentrations.

Supplementary material related to this article is available online at: http://www.atmos-chem-phys-discuss.net/13/9953/2013/ acpd-13-9953-2013-supplement.pdf.

References

Alastuey, A., Querol, X., Plana, F., Viana, M., Ruiz, C. R., Campa, A. S., Rosa, J., Mantilla, E., and Santos, S. G.: Identification and chemical characterization of industrial particulate matter sources in southwest Spain, J. Air Waste Manage., 56, 993–1006, 2006.

Andreae, M. O. and Rosenfeld, D.: Aerosol–cloud–precipitation interactions, part 1, the nature and sources of cloud-active aerosols, Earth-Sci. Rev., 89, 13–41, 2008.

Bardouki, H., Liakakou, H., Economou, C., Sciare, J., Smolik, J., Zdimal, V., Eleftheriadis, K., Lazaridis, M., and Mihalopoulos, N.: Chemical composition of size resolved atmospheric aerosols in the eastern Mediterranean during summer and winter, Atmos. Environ., 37, 195–208, 2003.

Beijing EPB (Beijing Municipal Environmental Protection Bureau): Beijing communiqué on environmental quality, 2001–2005, available at: http://www.bjee.org.cn, last access: 24 July 2006, 2005.

Birmili, W., Allen, A. G., Bary, F., and Harrison, R. M.: Trace metal concentrations and water solubility in size-fractionated atmospheric particles and influence of road traffic, Environ. Sci. Technol., 40, 1144–1153, 2006.

Cachier, H. and Ducret, J.: Influence of biomass burning on equatorial African rains, Nature, 352, 228–230, 1991.

Cao, J. J., Lee, S. C., Chow, J. C., Watson, J. G., Ho, K. F., Zhang, R. J., Jin, Z. D., Shen, Z. X., Chen, G. C., Kang, Y. M., Zou, S. C., Zhang, L. Z., Qi, S. H., Dai, M. H., Cheng, Y., and Hu., K.: Spatial and seasonal distributions of carbonaceous aerosols over China, J. Geophys. Res., 112, D22S11. doi:10.1029/2006JD008205, 2007.

Cao, J. J., Chow, J. C., Tao, J., Lee, S. C., Watson, J. G., Ho, K. F., Wang, G. H., Zhu, C. S., and Han, Y. M.: Stable carbon isotopes in aerosols from Chinese cities: influence of fossil fuels, Atmos. Environ., 45, 1359–1363, 2011.

Chan, C. K. and Yao, X. H.: Air Pollution in Mega Cities in China, Atmos. Environ., 42, 1–42, 2008.

Chen, L., Pryor, S. C., and Li, D. L.: Assessing the performance of Intergovernmental Panel on Climate Change AR5 climate models in simulating and projecting wind speeds over China, J. Geophys. Res., 117, D24102, doi:10.1029/2012JD017533, 2012.

Chen, W. Y. and Xu, R. N.: Clean coal technology development in China, Energ. Policy, 38, 2123–2130, 2010.

Chester, R.: Marine Geochemistry, Cambridge University Press, London, 698 pp., 1990.

Chow, J. C., Watson, J. G., Fujita, E. M., Lu, Z., and Lawson, D. R.: Temporal and spatial variation of $PM_{2.5}$ and PM_{10} aerosol in the Southern California air quality study, Atmos. Environ., 28, 2061–2080, 1994.

Chow, J. C., Watson, J. G., Lu, Z., Lowenthal, D. H., Frazier, C. A., Solomon, P. A., Thuillier, R. H., and Magliano, K.: Descriptive analysis of $PM_{2.5}$ and PM_{10} at regionally representative locations during SJVAQS/AUSPEX, Atmos. Environ., 30, 2079–2112, 1996.

Chow, J. C., Watson, J. G., Chen, L. W., Chang, M. C., Robinson, N. F., Trimble, D., and Kohl, S.: The IMPROVE_A temperature protocol for thermal/optical carbon analysis: maintaining consistency with a long-term database, J. Air Waste Manage., 42, 1014–1023, 2007.

Christian, T. J., Yokelson, R. J., Cárdenas, B., Molina, L. T., Engling, G., and Hsu, S.-C.: Trace gas and particle emissions from domestic and industrial biofuel use and garbage burning in central Mexico, Atmos. Chem. Phys., 10, 565–584, doi:10.5194/acp-10-565-2010, 2010.

Dall'Osto, M., Querol, X., Amato, F., Karanasiou, A., Lucarelli, F., Nava, S., Calzolai, G., and Chiari, M.: Hourly elemental concentrations in $PM_{2.5}$ aerosols sampled simultaneously at urban background and road site, Atmos. Chem. Phys. Discuss., 12, 20135–20180, doi:10.5194/acpd-12-20135-2012, 2012.

Dan, M., Zhuang, G. S., Li, X. X., Tao, H. R., and Zhuang, Y. H.: The characteristics of car-bonaceous species and their sources in $PM_{2.5}$ in Beijing, Atmos. Environ., 38, 3443–3452, 2004.

Dockery, D. W. and Pope, C. A.: Acute respiratory effects of particulate air pollution, Annu. Rev. Publ. Health, 15, 107–132, 1994.

Duan, F. K., Liu, X. D., He, K. B., Lu, Y. Q., and Wang, L.: Atmospheric aerosol concentration level and chemical characteristic of its water soluble ionic species in wintertime in Beijing, China, J. Environ. Monitor., 4, 569–573, 2003.

Duan, F. K., He, K. B., Ma, Y. L., Yang, F. M., Yu, X. C., Cadle, S. H., Chan, T., and Mulawa, P. A.: Concentration and chemical characteristics of $PM_{2.5}$ in Beijing, China: 2001–2002, Sci. Total Environ., 355, 264–275, 2006.

Eatough, D. J., Cui, W. X., Hull, J., and Farber, R. J.: Fine particulate chemical composition and light extinction at Meadview, AZ, J. Air Waste Manage., 56, 1694–1706, 2006.

Fang, M., Chan, C. K., and Yao, X. H.: Managing air quality in a rapidly developing nation: China, Atmos. Environ., 43, 79–86, 2009.

Gao, X., Yang, L., Cheng, S., Gao, R., Zhou, Y., Xue, L., Shou, Y., Wang, J., Wang, X., Nie, W., Xu, P., and Wang, W.: Semi-continuous measurement of water-soluble ions in $PM_{2.5}$ in Jinan, China: temporal variations and source apportionments, Atmos. Environ., 45, 6048–6056, 2011.

Gu, J. X., Bai, Z. P., Li, W. F., Wu, L. P., Liu, A. X., Dong, H. Y., and Xie, Y. Y.: Chemical composition of $PM_{2.5}$ during winter in Tianjin, China, Particuology, 9, 215–221, 2011.

Guinot, B., Cachier, H., and Oikonomou, K.: Geochemical perspectives from a new aerosol chemical mass closure, Atmos. Chem. Phys., 7, 1657–1670, doi:10.5194/acp-7-1657-2007, 2007.

Guo, S., Hu, M., Guo, Q. F., Zhang, X., Zheng, M., Zheng, J., Chang, C. C., Schauer, J. J., and Zhang, R. Y.: Primary sources and secondary formation of organic aerosols in Beijing, China, Environ. Sci. Technol., 46, 9846–9853, 2012.

Han, J. S., Moon, K. J., Lee, S. J., Kim, Y. J., Ryu, S. Y., Cliff, S. S., and Yi, S. M.: Size-resolved source apportionment of ambient particles by positive matrix factorization at Gosan background site in East Asia, Atmos. Chem. Phys., 6, 211–223, doi:10.5194/acp-6-211-2006, 2006.

Hao, J. M., Wang, L. T., Li, L., Hu, J. N., and Yu, X. C.: Air pollutants contribution and control strategies of energy-use related sources in Beijing, Sci. China Ser. D, 48, 138–146, 2005.

Chemical characterization and source apportionment

R. Zhang et al.

Title Page

Abstract	Introduction
Conclusions	References
Tables	Figures

|◄ | ►|

◄ | ►

Back | Close

Full Screen / Esc

Printer-friendly Version

Interactive Discussion

He, K. B., Yang, F. M., Ma, Y. L., Zhang, Q., Yao, X., Chan, C. K., Cadle, S., Chan, T., and Mulawa, P.: The Characteristics of PM$_{2.5}$ in Beijing, China, Atmos. Environ., 35, 4959–4970, 2001.

He, K. B., Huo, H., and Zhang, Q.: Urban air pollution in China: current status, characteristics, and progress, Annu. Rev. Energ. Env., 27, 397–431, 2002.

He, S. Z., Chen, Z. M., Zhang, X. Zhao, Y., Huang, D. M., Zhao, J. N., Zhu, T., Hu, M., and Zeng, L. M.: Measurement of atmospheric hydrogen peroxide and organic peroxides in Beijing before and during the 2008 Olympic Games: chemical and physical factors influencing their concentrations, J. Geophys. Res., 115, D17307, doi:10.1029/2009JD013544, 2010.

He, X., Li, C. C., Lau, A. K. H., Deng, Z. Z., Mao, J. T., Wang, M. H., and Liu, X. Y.: An intensive study of aerosol optical properties in Beijing urban area, Atmos. Chem. Phys., 9, 8903–8915, doi:10.5194/acp-9-8903-2009, 2009.

Ho, K. F., Lee, S. C., Cao, J. J., Chow, J. C., Watson, J. G., and Chan, C. K.: Seasonal variations and mass closure analysis of particulate matter in Hong Kong, Sci. Total Environ., 355, 276–287, 2006.

Hopke, P. K.: Recent developments in receptor modeling, J. Chemometr., 17, 255–265, 2003.

Hsu, S. C., Liu, S. C., Kao, S. J., Jeng, W. L., Huang, Y. T., Tseng, C. M., Tsai, F., Tu, J. Y., and Yang, Y.: Water soluble species in the marine aerosol from the Northern South China sea: High chloride depletion related to air pollution, J. Geophys. Res., 112, D19304, doi:10.1029/2007JD008844, 2007.

Hsu, S. C., Liu, S. C., Huang, Y. T., Lung, S. C. C., Tsai, F., Tu, J. Y., and Kao, S. J: A criterion for identifying Asian dust events based on Al concentration data collected from Northern Taiwan between 2002 and early 2007, J. Geophys. Res., 113, D18306, doi:10.1029/2007JD009574, 2008.

Hsu, S. C., Liu, S. C., Huang, Y. T., Chou, C. C. K., Lung, S. C. C., Liu, T. H., Tu, J. Y., and Tsai, F.: Long-range southeastward transport of Asian biosmoke pollution: signature detected by aerosol potassium in Northern Taiwan, J. Geophys. Res., 114, D14301, doi:10.1029/2009JD011725, 2009.

Hsu, S. C., Liu, S. C., Tsai, F., Engling, G., Lin, I. I., Chou, C. K. C., Kao, S. J., Lung, S. C. C., Chan, C. Y., Lin, S. C., Huang, J. C., Chi, K. H., Chen, W. N., Lin, F. J., Huang, C. H., Kuo, C. L., Wu, T. C., and Huang, Y. T.: High wintertime particulate matter pollution over an offshore island (Kinmen) off southeastern China: an overview, J. Geophys. Res., 115, D17309, doi:10.1029/2009JD013641, 2010a.

Hsu, S. C., Liu, S. C., Arimoto, R., Shiah, F. K., Gong, G. C., Huang, Y. T., Kao, S. J., Chen, J. P., Lin, F. J., Lin, C. Y., Huang, J. C., Tsai, F., and Lung, S. C. C.: Effects of acidic processing, transport history, and dust and sea salt loadings on the dissolution of iron from Asian dust, J. Geophys. Res., 115, D19313, doi:10.1029/2009JD013442, 2010b.

Hsu, Y. K., Holsen, T. M., and Hopke, P. K.: Comparison of hybrid receptor models to locate PCB sources in Chicago, Atmos. Environ., 37, 545–562, 2003.

Hu, M., Zhou, F. M., Shao, K. S., Zhang, Y. H., Tang, X. Y. and Slanina, J.: Diurnal variations of aerosol chemical compositions and related gaseous pollutants in Beijing and Guangzhou, J. Environ. Sci. Heal. A., 37, 479–488, 2002a.

Hu, M., He, L. Y., Zhang, Y. H., Wang, M., Kim, Y. P., and Moon, K. C.: Seasonal variation of ionic species in fine particles at Qingdao, China, Atmos. Environ., 36, 5853–5859, 2002b.

Hueglin, C., Gehrig, R., Baltensperger, U., Gysel, M., Monn, C., and Vonmont, H.: Chemical characterisation of $PM_{2.5}$, PM_{10} and coarse particles at urban, near-city and rural sites in Switzerland., Atmos. Environ., 39, 637–651, 2005.

Ianniello, A., Spataro, F., Esposito, G., Allegrini, I., Hu, M., and Zhu, T.: Chemical characteristics of inorganic ammonium salts in $PM_{2.5}$ in the atmosphere of Beijing (China), Atmos. Chem. Phys., 11, 10803–10822, doi:10.5194/acp-11-10803-2011, 2011.

IPCC: Climate Change 2007–Synthesis Report, Contribution of Working Groups I, II, and III to the Fourth Assessment Report of the Intergovernmental Panel on Climate Change (IPCC, Geneva, Switzerland, 2007), 2007.

Landis, M. S., Norris, G. A., Williams, R. W., and Weinstein, J. P.: Personal exposures to $PM_{2.5}$ mass and trace elements in Baltimore, MD, USA, Atmos. Environ., 35, 6511–6524, 2001.

Lee, E., Chan, C. K., and Paatero, P.: Application of positive matrix factorization in source apportionment of particulate pollutants in Hong Kong, Atmos. Environ., 33, 3201–3212, 1999.

Lee, K. H., Li, Z. Q., Cribb, M. C., Liu, J. J., Wang, L., Zheng, Y. F., Xia, X. A., Chen, H. B., and Li, B.: Aerosol optical depth measurements in eastern China and a new calibration method, J. Geophys. Res., 115, D00K11, doi:10.1029/2009JD012812, 2010.

Li, G., Chen, J., Chen, Y., Yang, J., Ji, J., and Liu, L.: Dolomite as a tracer for the source regions of Asian dust, J. Geophys. Res., 112, D17201, doi:10.1029/2007JD008676, 2007.

Li, W. J. and Shao, L. Y.: Observation of nitrate coatings on atmospheric mineral dust particles, Atmos. Chem. Phys., 9, 1863–1871, doi:10.5194/acp-9-1863-2009, 2009.

Liu, J. and Diamond, J.: China's environment in a globalizing world, Nature, 435, 1179–1186, 2005.

Mahowald, N.: Aerosol indirect effect on biogeochemical cycles and climate, Science, 334, 794–796, 2011.

Malm, W. C., Sisler, J. F., Huffman, D., Eldred, R. A., and Cahill, T. A.: Spatial and seasonal trends in particle concentration and optical extinction in the United States, J. Geophys. Res., 99, 1347–1370, 1994.

Malm, W. C., Day, D. E., Carrico, C., Kreidenweis, S. M., Collett, Jr. J. L., McMeeking, G., Lee, T., Carrillo, J., and Schichtel, B.: Intercomparison and closure calculations using measurements of aerosol species and optical properties during the yosemite aerosol characterization study, J. Geophys. Res., 110, doi:10.1029/2004JD005494, D14302, 2005.

Marani, D., Braguglia, C. M., Mininni, G., and Maccioni, F.: Behaviour of Cd, Cr, Mn, Ni, Pb, and Zn in sewage sludge incineration by fluidised bed furnace, Waste Manage., 23, 117–124, 2003.

Mukai, H., Tanaka, A., Fujii, T., Zeng, Y., Hong, Y., Tang, J., Guo, S., Xue, H., Sun, Z., Zhou, J., Xue, D., Zhao, J., Zhai, G., Gu, J., and Zhai, P.: Regional characteristics of sulphur and lead isotope ratios in the atmosphere at several Chinese urban sites, Environ. Sci. Technol., 35, 1064–1071, 2001.

Niwa, Y., Hiura, Y., Murayama, T., Yokode, M., and Iwai, N.: Nano-sized carbon black exposure exacerbates atherosclerosis in ldl-receptor knockout mice, Circ. J., 71, 1157–1161, 2007.

Oberdörster, G.: Pulmonary effects of inhaled ultrafine particles, Int. Arch. Occ. Env. Hea., 74, 1–8, 2001.

Okuda, T., Matsuura, S., Yamaguchi, D., Umemura, T., Hanada, E., Orihara, H., Tanaka, S., He, K. B., Ma, Y. L., Cheng, Y., and Liang, L. L.: The impact of the pollution control measures for the 2008 Beijing Olympic Games on the chemical composition of aerosols, Atmos. Environ., 45, 2789–2794, 2011.

Pathak, R. K., Yao, X. H., Lau, A. K. H., and Chan, C. K.: Sampling artifacts of acidity and ionic species in $PM_{2.5}$, Sci. Total Environ., 38, 254–259, 2004.

Pirrone, N., Cinnirella, S., Feng, X., Finkelman, R. B., Friedli, H. R., Leaner, J., Mason, R., Mukherjee, A. B., Stracher, G. B., Streets, D. G., and Telmer, K.: Global mercury emissions to the atmosphere from anthropogenic and natural sources, Atmos. Chem. Phys., 10, 5951–5964, doi:10.5194/acp-10-5951-2010, 2010.

Polissar, A. V., Hopke, P. K., Paatero, P., Kaufmann, Y. J., Hall, D. K., Bodhaine, B. A., Dutton, E. G., and Harris, J. M.: The aerosol at Barrow, Alaska: Long-term trends and source locations, Atmos. Environ., 33, 2441–2458, 1999.

Pope, C. A., Thun, M. J., Namboodiri, M. M., Dockery, D. W., Evans, J. S., Speizer, F. E., and Heath, C. W. Jr.: Particulate air pollution as a predictor of mortality in a prospective study of US adults, Am. J. Resp. Crit. Care, 151, 669–674, 1995.

Pósfai, M., Gelencsér, A., Simonics, R., Arató, K., Li, J., Hobbs, P. V., and Buseck, P. R.: Atmospheric tar balls: particles from biomass and biofuel burning, J. Geophys. Res., 109, D06213, doi:10.1029/2003JD004169, 2004.

Qian, W. and Lin, X.: Regional trends in recent precipitation indices in China, Meteorol. Atmos. Phys., 90, 193–207, 2005.

Qian, W. H., Quan, L. S., and Shi, S. Y.: Variations of the dust storm in china and its climatic control, J. Climate, 15, 1216–1229, 2002.

Ramanathan, V. and Feng, Y.: Air pollution, greenhouse gases and climate change: global and regional perspectives, Atmos. Environ., 43, 37–50, 2009.

Rees, S. L., Robinson, A. L., Khlystov, A., Stanier, C. O., and Pandis, S. N.: Mass balance closure and the Federal Reference Method for $PM_{2.5}$ in Pittsburgh, PA, Atmos. Environ., 38, 3305–3318, 2004.

Schwartz, J., Dockery, D. W., and Neas, L. M.: Is daily mortality associated specifically with fine particles?, J. Air Waste Manage., 46, 927–939, 1996.

Seinfeld, J. H.: Urban air pollution: state of the science, Science, 243, 745–752, 1989.

Shao, M., Tang, X. Y., Zhang, Y. H., and Li, W. J.: City clusters in China: air and surface water pollution, Front. Ecol. Environ., 4, 353–361, 2006.

Shen, Z. X., Cao, J. J., Arimoto, R., Han, Y. M., Zhu, C. S., Tian, J., and Liu, S. X.: Chemical characteristics of fine particles (PM_1) from Xi'an, China, Aerosol Sci. Tech., 44, 461–472, 2010.

Song, S. J., Wu, Y., Jiang, J. K. Yang, L., Cheng, Y., and Hao, J. M.: Chemical characteristics of size-resolved $PM_{2.5}$ at a roadside environment in Beijing, China, Environ. Pollut., 161, 215–221, 2012.

Song, Y., Zhang, Y. H., Xie, S. D., Zeng, L. M., Zheng, M., Salmon, L. G., Shao, M., and Slanina, S.: Source apportionment of $PM_{2.5}$ in Beijing by positive matrix factorization, Atmos. Environ., 40, 1526–1537, 2006.

Song, Y., Tang, X. Y., Xie, S. D., Zhang, Y. H., Wei, Y. J., Zhang, M. S., Zeng, L. M., and Lu, S. H.: Source apportionment of $PM_{2.5}$ in Beijing in 2004, J. Hazard. Mater., 146, 124–130, 2007.

Song, Y., Miao, W. J., Liu, B., Dai, W., and Cai, X. H.: Identifying anthropogenic and natural influences on extreme pollution of respirable suspended particulates in Beijing using backward trajectory analysis, J. Hazard. Mater., 154, 459–468, 2008.

Speer, R. E., Barnes, H. M., and Brown, R.: An instrument for measuring the liquid water content of aerosols, Aerosol Sci. Tech., 27, 50–61, 1997.

Streets, D. G., Wu, Y., and Chin, M.: Two-decadal aerosol trends as a likely explanation of the global dimming/brightening transition, Geophys. Res. Lett., 33, L15806, doi:10.1029/2006GL026471, 2006.

Streets, D. G., Fu, J. S., Jang, C. J., Hao, J. M., He, K. B., Tang, X. Y., Zhang, Y. H., Wang, Z. F., Li, Z. P., Zhang, Q., Wang, L. T., Wang, B. Y., and Yu, C.: Air quality during the 2008 Beijing Olympic Games, Atmos. Environ., 41, 480–492, 2007.

Sun, J., Zhang, M., and Liu, T.: Spatial and temporal characteristics of dust storms in China and its surrounding regions, 1960–1999: Relations to source area and climate, J. Geophys. Res., 106, 10325–10333, 2001.

Sun, Y., Zhuang, G., Tang, A., Wang, Y., and An, Z.: Chemical characteristics of $PM_{2.5}$ and PM_{10} in haze-Fog episodes in Beijing, Environ. Sci. Technol., 40, 3148–3155, 2006.

Takuwa, T., Mkilaha, I. S. N., and Naruse, I.: Mechanisms of fine particulates formation with alkali metal compounds during coal combustion, Fuel, 85, 671–678, 2006.

Tao, J., Ho, K. F., Chen, L., Zhu, L., Han, J., and Xu, Z.: Effect of chemical composition of $PM_{2.5}$ on visibility in Guangzhou, China, 2007 spring, Particuology, 7, 68–75, 2009.

Taylor, S. R.: Trace element abundances and the chondritic Earth model, Geochim. Cosmochim. Ac., 28, 1989–1998, 1964.

Tian, H., Gao, J., Lu, L., Zhao, D., Cheng, K., and Qiu, P.: Temporal trends and spatial variation characteristics of hazardous air pollutant emission inventory from municipal solid waste incineration in China, Environ. Sci. Technol., 46, 10364–10371, 2012.

Tsai, Y. I. and Kuo, S. C.: $PM_{2.5}$ aerosol water content and chemical composition in a metropolitan and a coastal area in southern Taiwan, Atmos. Environ., 39, 4827–4839, 2005.

Turpin, B. J. and Lim, H. J.: Species contributions to $PM_{2.5}$ mass concentrations: revisiting common assumptions for estimating organic mass, Aerosol Sci. Tech., 35, 602–610, 2001.

Viidanoja, J., Sillanpaa, M., Laakia, J., Kerminen, V. M., Hillamo, R., Aarnio, P., and Koskentalo, T.: Organic and black carbon in $PM_{2.5}$ and PM_{10}: 1 year of data from an urban site in Helsinki, Finland, Atmos. Environ., 36, 3183–3193, 2002.

Wåhlin, P., Berkowicz, R., and Palmgren, F.: Characterisation of traffic-generated particulate matter in Copenhagen, Atmos. Environ., 40, 2151–2159, 2006.

Wang, H. L., Zhuang, Y. H., Wang, Y., Sun, Y. L., Yuan, H., Zhuang, G. S., and Hao, Z. P.: Long-term monitoring and source apportionment of $PM_{2.5}/PM_{10}$ in Beijing, China, J. Environ. Sci., 20, 1323–1327, 2008.

Wang, Y., Zhuang, G. S., Tang, A. H., Yuan, H., Sun, Y. L., Chen, S., and Zheng, A. H.: The ion chemistry and the source of $PM_{2.5}$ aerosol in Beijing, Atmos. Environ., 39, 3771–3784, 2005.

Wang, Y. Q., Zhang, X. Y., Arimoto, R., Cao, J. J., and Shen, Z. X.: The transport pathways and sources of PM_{10} pollution in Beijing during spring 2001, 2002 and 2003, Geophys. Res. Lett., 31, L14110, doi:10.1029/2004GL019732, 2004.

Watson, J. G.: Visibility: science and regulation, J. Air Waste Manage., 52, 628–713, 2003.

Watson, J. G. and Chow, J. C.: CMB8 Applications and Validation Protocol for $PM_{2.5}$ and VOCs, Desert Research Institute Report, No. 1808.2D1, Prepared for U.S. Environmental Protection Agency, Research Triangle Park, NC, Desert Research Institute, Reno, NV, 1998.

Watson, J. G. and Chow, J. C.: $PM_{2.5}$ chemical source profiles for vehicular exhaust, vegetation burning, geological materials and coal burning in Northwestern Colorado during 1995, Chemosphere, 43, 1141–1151, 2001.

WHO: World Health Organization Air Quality Guidelines Global Update, E87950, Geneva, Switzerland , 2005.

Widory, D., Liu, X. D., and Dong, S. P.: Isotopes as tracers of sources of lead and strontium in aerosols (TSP and $PM_{2.5}$) in Beijing, Atmos. Environ., 44, 3679–3687, 2010.

Xia, X. A., Chen, H. B., Wang, P. C., Zhang, W. X., Goloub, P., Chatenet, B., Eck, T. F., and Holben, B. N.: Variation of column-integrated aerosol properties in a Chinese urban region, J. Geophys. Res., 111, D05204, doi:10.1029/2005JD006203, 2006.

Xie, S. D., Liu, Z., Chen, T., and Hua, L.: Spatiotemporal variations of ambient PM_{10} source contributions in Beijing in 2004 using positive matrix factorization, Atmos. Chem. Phys., 8, 2701–2716, doi:10.5194/acp-8-2701-2008, 2008.

Xing, L., Fu, T.-M., Cao, J. J., Lee, S. C., Wang, G. H., Ho, K. F., Cheng, M.-C., You, C.-F., and Wang, T. J.: Seasonal and spatial variability of the organic matter-to-organic carbon mass ratios in Chinese urban organic aerosols and a first report of high correlations between aerosol oxalic acid and zinc, Atmos. Chem. Phys. Discuss., 13, 1247–1277, doi:10.5194/acpd-13-1247-2013, 2013.

Title Page

Abstract | Introduction

Conclusions | References

Tables | Figures

◀ | ▶

◀ | ▶

Back | Close

Full Screen / Esc

Printer-friendly Version

Interactive Discussion

Yan, P., Zhang, R. J., Huan, N., Zhou, X. J., Zhang, Y. M., Zhou, H. G., and Zhang, L. M.: Characteristics of aerosols and mass closure study at two WMO GAW regional background stations in eastern China, Atmos. Environ., 60, 121–131, 2012.

Yao, Q., Li, S. Q., Xu, H. W., Zhuo, J. K., and Song, Q.: Studies on formation and control of combustion particulate matter in China: a review, Energy, 34, 1296–1309, doi:10.1016/j.energy.2009.03.013, 2009.

Yao, X., Lau, A. P. S., Fang, M., Chan, C. K., and Hu, M.: Size distribution and formation of ionic species in atmospheric particulate pollutants in Beijing, China, Atmos. Environ., 37, 2991–3000, 2003.

Yao, X. H., Chan, C. K., Fang, M., Cadle, S., Chan, T., Mulawa, P., He, K. B., and Ye, B. M.: The water-soluble ionic composition of $PM_{2.5}$ in Shanghai and Beijing, China, Atmos. Environ., 36, 4223–4234, 2002.

Yassaa, N., Meklati, B. Y., Cecinato, A., and Marino, F.: Organic aerosols in urban and waste landfill of Algiers metropolitan area: occurrence and sources, Environ. Sci. Technol., 35, 306–311, 2001.

Yu, L. D., Wang, G. F., Zhang, R. J., Zhang, L. M., Song, Y., Wu, B. B., Li, X. F., An, K., and Chu, J. H.: Characterization and source apportionment of $PM_{2.5}$ in an urban environment in Beijing, Aerosol Air Qual. Res., 13, 574–583, 2013.

Yu, Y., Schleicher, N., Norra, S., Fricker, M., Dietze, V., Kaminski, U., Cena, K., and Stüben, D.: Dynamics and origin of $PM_{2.5}$ during a three-year sampling period in Beijing, China, J. Environ. Monitor., 13, 334–346, 2011.

Zhang, D. and Iwasaka, Y.: Nitrate and sulfate in individual Asian dust-storm particles in Beijing, China in spring of 1995 and 1996, Atmos. Environ., 33, 3213–3223, 1999.

Zhang, Q., He, K., and Huo, H.: Cleaning China's air, Nature, 484, 161–162, 2012.

Zhang, R. J., Wang, M. X., Zhang, X. Y., and Zhu, G.: Analysis on the chemical and physical properties of particles in a dust storm in spring in Beijing, Powder Technol., 137, 77–82, 2003.

Zhang, R. J., Cao, J. J., Lee, S. C., Shen, Z. X., and Ho, K. F.: Carbonaceous aerosols in PM_{10} and pollution gases in winter in Beijing, J. Environ. Sci., 19, 564–571, 2007.

Zhang, R. J., Tao, J., Ho, K. F., Shen, Z. X., Wang, G. H., Cao, J. J., Liu, S. X., Zhang, L. M., and Lee, S. C.: Characterization of atmospheric organic carbon and elemental carbon of $PM_{2.5}$ in a typical semi-arid area of northeastern China, Aerosol Air Qual. Res., 12, 792–802, doi:10.4209/aaqr.2011.07.0110, 2012.

Zhang, X. Y., Arimoto, R., and An, Z. S.: Dust emission from Chinese desert sources linked to variations in atmospheric circulation, J. Geophys. Res., 102, 28041–28047, 1997.

Zhang, X. Y., Gong, S. L., Shen, Z. X., Mei, F. M., Xi, X. X., Liu, L. C., Zhou, Z. J., Wang, D., Wang, Y. Q., and Cheng, Y.: Characterization of soil dust aerosol in China and its transport and distribution during 2001 ACE-Asia: 1. network observations, J. Geophys. Res., 108, D94261, doi:10.1029/2002JD002632, 2003.

Zhang, X. Y., Wang, Y. Q., Zhang, X. C., Guo, W., and Gong, S. L.: Carbonaceous aerosol composition over various regions of China during 2006, J. Geophys. Res., 113, D14111, doi:10.1029/2007JD009525, 2008.

Zhang, X. Y., Zhuang, G. S., Yuan, H., Rahn, K. A., Wang, Z. F., and An, Z. S.: Aerosol particles from dried salt-lakes and saline soils carried on dust storms over Beijing, Terr. Atmos. Ocean. Sci., 20, 619–628, 2009.

Zhang, Y. P., Wang, X. F., Chen, H., Yang, X., Chen, J. M., and Allen, J. O.: Source apportionment of lead-containing aerosol particles in Shanghai using single particle mass spectrometry, Chemosphere, 74, 501–507, 2009.

Zheng, X. Y., Liu, X. D., Zhao, F. H., Duan, F. K., Yu, T., and Cachier, H.: Seasonal characteristics of biomass burning contribution to Beijing aerosol, Sci. China Ser. B, 48, 481–488, 2005.

Zhou, J. M., Zhang, R. J., Cao, J. J., Chow, J. C., and Watson, J. G.: Carbonaceous and ionic components of atmospheric fine particles in Beijing and their impact on atmospheric visibility, Aerosol Air Qual. Res., 12, 492–502, 2012.

Title Page

Abstract | Introduction

Conclusions | References

Tables | Figures

◀ | ▶

◀ | ▶

Back | Close

Full Screen / Esc

Printer-friendly Version

Interactive Discussion

Table 1. Statistical summary showing the means (with one standard deviation) and ranges of atmospheric concentrations for PM$_{2.5}$ (in μg m^{-3}) and selected species (in ng m^{-3}) in the entire sampling (annual) and four season (months) periods.

Species	Annual	Spring	Summer	Autumn	Winter
PM$_{2.5}$	135 ± 63	126 ± 59	138 ± 48	135 ± 55	139 ± 86
	39–355	39–280	41–226	45–251	48–355
SO$_4^{2-}$	13.6 ± 12.4	14.7 ± 11.5	23.5 ± 14.5	7.9 ± 7.4	8.5 ± 8.6
	0.9–52.8	2.3–52.8	2.5–52.0	0.9–25.7	1.3–34.4
NO$_3^-$	11.3 ± 10.8	15.5 ± 13.7	11.8 ± 8.2	10.7 ± 11.0	7.3 ± 8.1
	0.3–63.8	1.3–63.8	1.8–31.5	0.3–34.7	1.6–35.5
NH$_4^+$	6.9 ± 7.1	7.5 ± 8.1	11.0 ± 6.9	4.7 ± 5.8	4.5 ± 5.7
	0.1–39.1	0.6–39.1	0.5–23.9	0.1–17.7	0.3–23.3
Cl$^-$	1.42 ± 2.18	0.72 ± 0.81	0.30 ± 0.56	1.12 ± 0.98	3.52 ± 3.32
	0.03–10.34	0.04–3.74	0.03–3.06	0.09–3.71	0.19–10.34
Na$^+$	0.46 ± 0.55	0.31 ± 0.18	0.17 ± 0.09	0.30 ± 0.22	1.08 ± 0.80
	0.04–2.82	0.08–0.94	0.04–0.42	0.05–1.06	0.11–2.82
K$^+$	0.92 ± 0.75	1.08 ± 0.71	0.66 ± 0.47	1.13 ± 0.90	0.81 ± 0.77
	0.03–3.66	0.14–3.14	0.20–2.47	0.03–3.66	0.05–2.53
Mg^{2+}	0.16 ± 0.13	0.24 ± 0.20	0.07 ± 0.03	0.16 ± 0.07	0.18 ± 0.09
	0.02–1.04	0.03–1.04	0.02–0.16	0.06–0.31	0.06–0.45
Ca^{2+}	1.6 ± 1.5	2.6 ± 2.2	0.6 ± 0.3	1.7 ± 1.0	1.5 ± 0.9
	0.2–11.3	0.2–11.3	0.2–1.7	0.5–4.2	0.5–4.0
Al	1.8 ± 1.5	2.5 ± 1.7	0.7 ± 0.4	2.0 ± 1.4	2.1 ± 1.5
	0.1–6.9	0.3–6.6	0.1–2.0	0.3–6.7	0.7–6.9
OC	16.9 ± 10.0	13.7 ± 4.4	11.1 ± 1.8	17.8 ± 5.6	24.9 ± 15.6
	5.9–58.6	5.9–23.7	7.4–16.6	7.5–26.2	8.5–58.6
EC	5.0 ± 4.4	2.8 ± 1.1	4.2 ± 1.2	5.3 ± 2.8	7.5 ± 7.4
	0.6–28.1	0.6–5.8	1.5–6.8	1.3–12.1	1.2–28.1

R. Zhang et al.

Table 2. Relative contributions from six identified sources of PM$_{2.5}$ in Beijing within the one-year and four-season periods.

Source	Spring	Summer	Autumn	Winter	Annual
Soil dust	23 %	3 %	18 %	16 %	15 %
Coal combustion	5 %	1 %	7 %	57 %	18 %
Biomass burning	19 %	6 %	17 %	7 %	12 %
Traffic and waste incineration emission	5 %	4 %	4 %	2 %	4 %
Industrial pollution	14 %	32 %	42 %	12 %	25 %
SIA	34 %	54 %	13 %	6 %	26 %

Table 3. Mean concentrations (in $\mu g\,m^{-3}$) of PM$_{2.5}$ and selected aerosol speciations in the identified trajectory clusters within the one-year (annual) and four season period. Also given are the percentages of each trajectory cluster classified in the one-year and four season periods. For details on trajectory clustering, please refer to the text.

Air-mass type	Annual					Spring				Summer				Autumn			Winter	
	NW$_s$	NW$_f$	N	E	S	NW$_s$	N	E	S	NW$_s$	N	E	S	NW$_f$	E	S	NW$_f$	E
Percent (%)	11.9	32.4	7.4	14.6	33.7	8.7	29.6	17.4	44.3	9.6	8.7	8.7	73.	49.6	26.8	23.6	88.2	11.8
PM$_{2.5}$	148	111	87	110	172	145	70	108	167	108	110	63	155	113	144	173	131	209
Sulfate	10.2	5	6.3	10.9	25.4	11.9	4.8	13.6	23.1	11.1	9.6	7.6	28.3	4.8	10.9	11.2	7	19.5
Nitrate	11.2	5.1	4.3	10.2	19.2	14	4.8	14.4	24.4	4.5	4	3.5	14.3	6.4	13.4	16.9	6.3	14.9
Ammonium	5.4	2.3	2.3	5.7	13.2	4.7	1.7	8	12.2	4.8	3.7	3.4	13.4	2.4	6.5	7.6	3.7	10.9
OC	22.2	18.1	10.8	13.8	16.4	15.5	10	11.5	16.7	12.4	12.2	9.4	11	15.6	18.7	21.6	23.8	33.6
EC	6.5	4.9	2.5	3.7	5.4	3.7	1.9	2.2	3.4	3.5	3.6	2.6	4.5	4	5.9	7.5	7	11.4
Mineral	31.3	36.5	26	16.4	20.8	64.8	32.8	15.3	39.1	15	21	4.8	8.5	33.3	19.4	30.4	31.3	21.8

Discussion Paper | Discussion Paper | Discussion Paper | Discussion Paper

ACPD

13, 9953–10007, 2013

Chemical characterization and source apportionment

R. Zhang et al.

Title Page

Abstract | Introduction

Conclusions | References

Tables | Figures

◄ | ►

Back | Close

Full Screen / Esc

Printer-friendly Version

Interactive Discussion
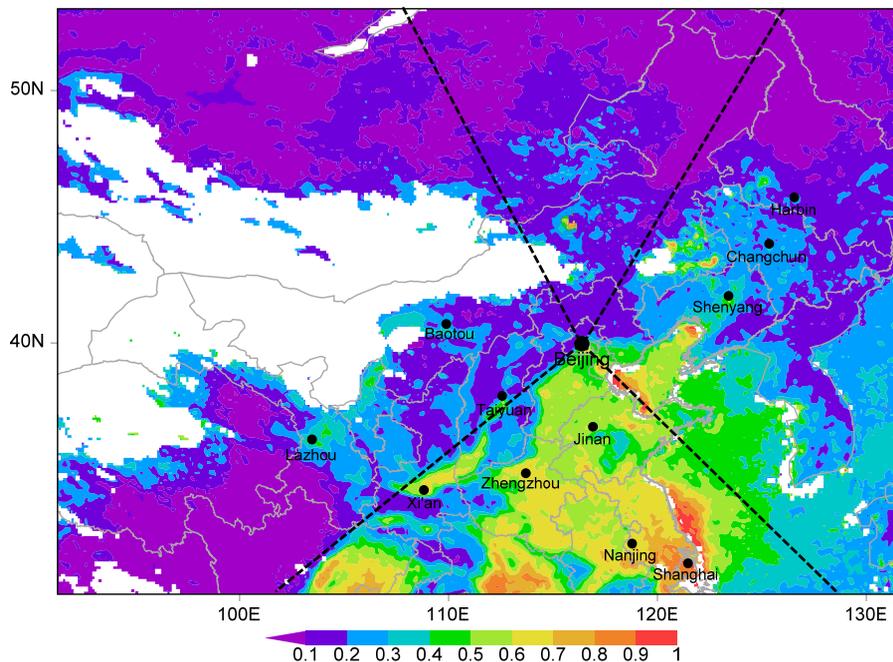
Fig. 1. Sampling location (116.30° E, 39.99° N) on a regional map superimposed with spatial distribution of annual mean fine aerosol optical depth (AOD) retrieved from MODIS satellite remote sensing in 2009. Dashed lines define four regions based on the trajectory clustering results discussed in Sect. 4.2 (seen in the text). Also shown are several major cities around Beijing.
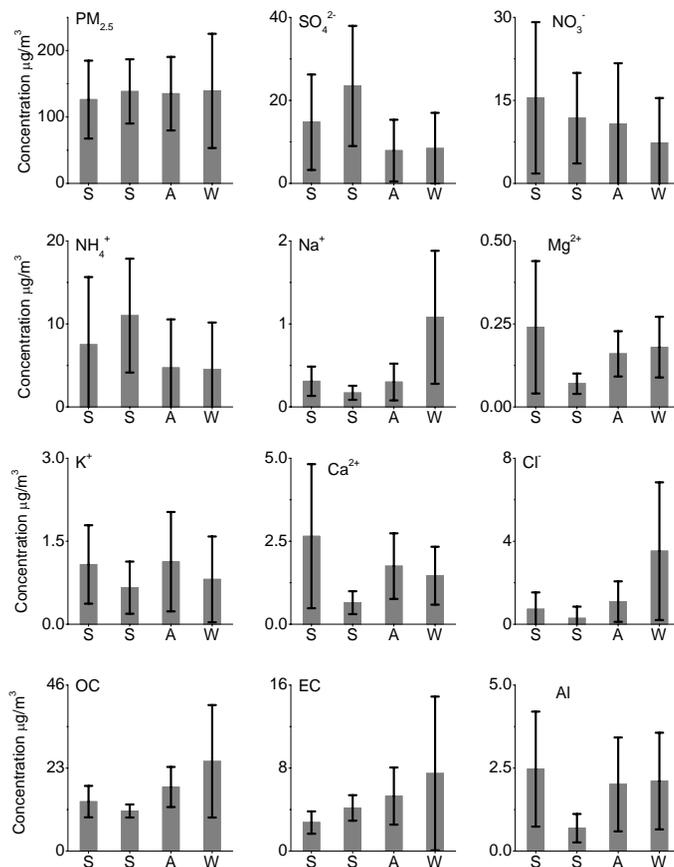
Fig. 2. Seasonal variations of PM$_{2.5}$ mass concentration and associated species, including SO$_4^{2-}$, NO$_3^-$, NH$_4^+$, Na$^+$, Mg^{2+}, K$^+$, Ca$_2^+$, Cl$^-$, OC, EC, and Al concentrations. Shown here are the mean and one standard deviation for each bar.

Title Page

Abstract | Introduction

Conclusions | References

Tables | Figures

◄ | ►◄

◄ | ►

Back | Close

Full Screen / Esc

Printer-friendly Version

Interactive Discussion
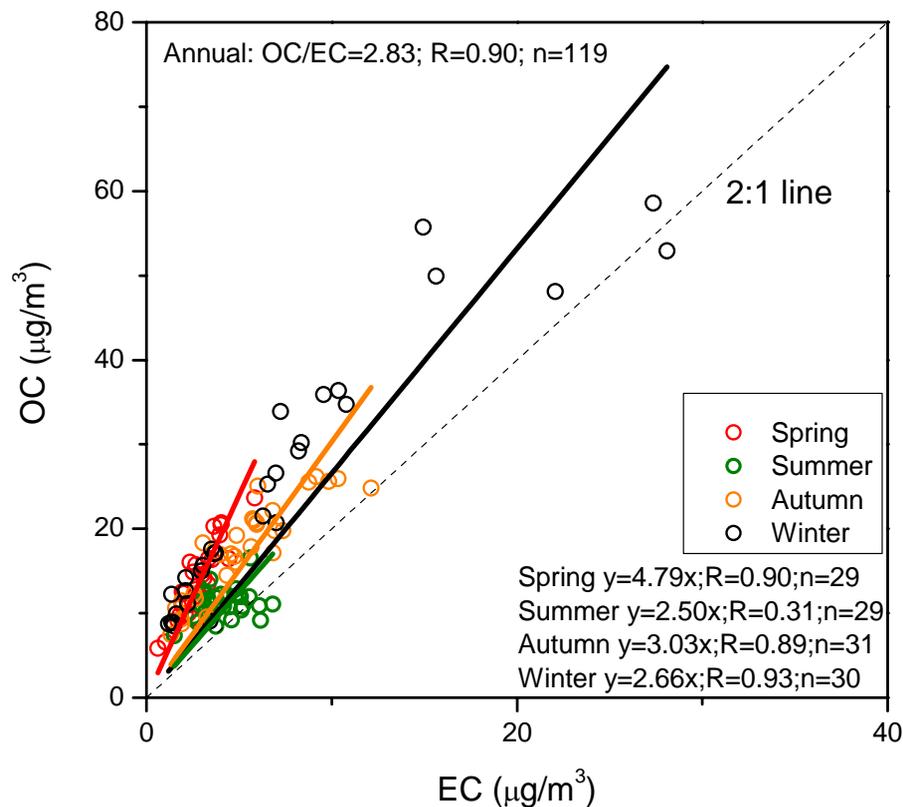
Fig. 3. Scatter plot showing the correlation between OC (y-axis) and EC (x-axis) in $PM_{2.5}$ collected from Beijing. Different symbols denote the four seasons. Linear regression equations are given in the annual and seasonal cases.

Title Page

Abstract | Introduction

Conclusions | References

Tables | Figures

|◄ | ►|

◄ | ►

Back | Close

Full Screen / Esc

Printer-friendly Version

Interactive Discussion
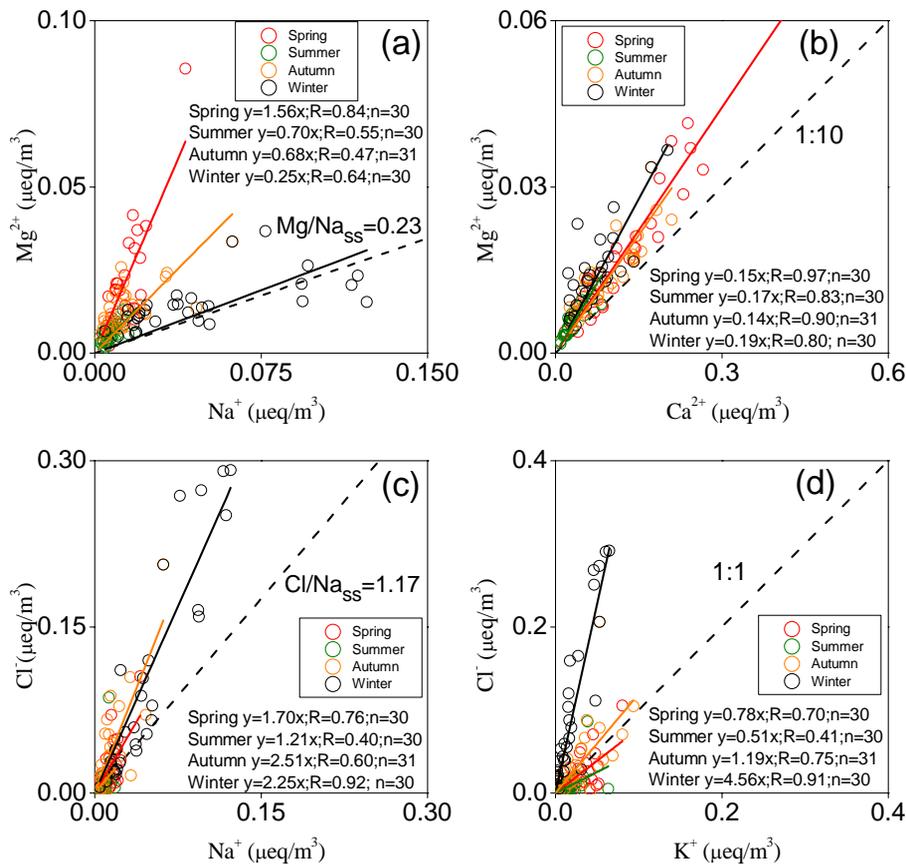
Fig. 4. Correlations between certain cations and anions: **(a)** Mg^{2+} versus Na^+, **(b)** Mg^{2+} versus Ca^{2+}, **(c)** Cl^- versus Na^+, and Cl^- versus K^+. Four seasons are considered and represented by different color symbols. Linear regression equations are also given. In panels **(a)** and **(c)**, the dashed lines indicate the Mg/Na and Cl/Na equivalent concentration ratios in seawater (sea salt), respectively.

Title Page

Abstract | Introduction

Conclusions | References

Tables | Figures

|◀ | ▶|

◀ | ▶

Back | Close

Full Screen / Esc

Printer-friendly Version

Interactive Discussion
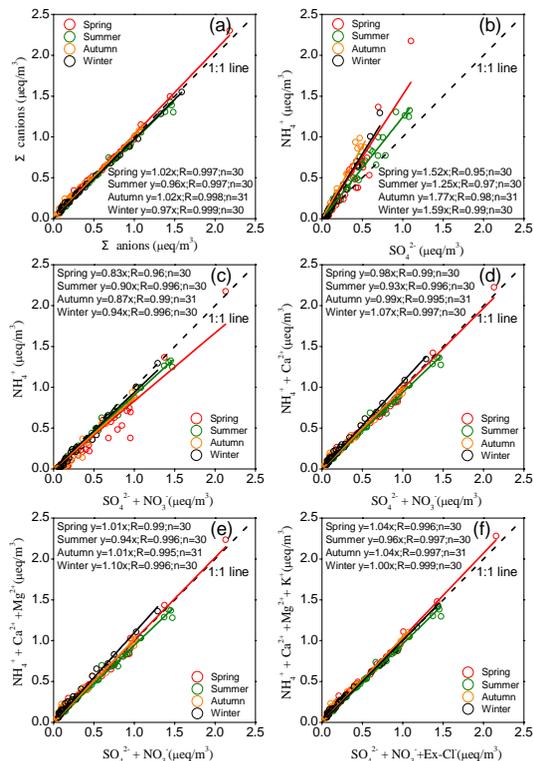
Fig. 5. Same as Fig. 4, but for **(a)** total cations versus total anions, **(b)** NH_4^+ versus SO_4^{2-}, **(c)** NH_4^+ versus $[SO_4^{2-} + NO_3^-]$, **(d)** $[NH_4^+ + Ca^{2+}]$ versus $[SO_4^{2-} + NO_3^-]$, **(e)** $[NH_4^+ + Ca^{2+} + Mg^{2+}]$ versus $[SO_4^{2-} + NO_3^-]$, and **(f)** $[NH_4^+ + Ca^{2+} + Mg^{2+}]$ versus $[SO_4^{2-} + NO_3^- + Ex-Cl^-]$. The detailed definition of $Ex-Cl^-$ (excessive-Cl^-) can be found in the text. The 1 : 1 lines are given for comparison.

Title Page

Abstract | Introduction

Conclusions | References

Tables | Figures

◄ | ►

◄ | ►

Back | Close

Full Screen / Esc

Printer-friendly Version

Interactive Discussion
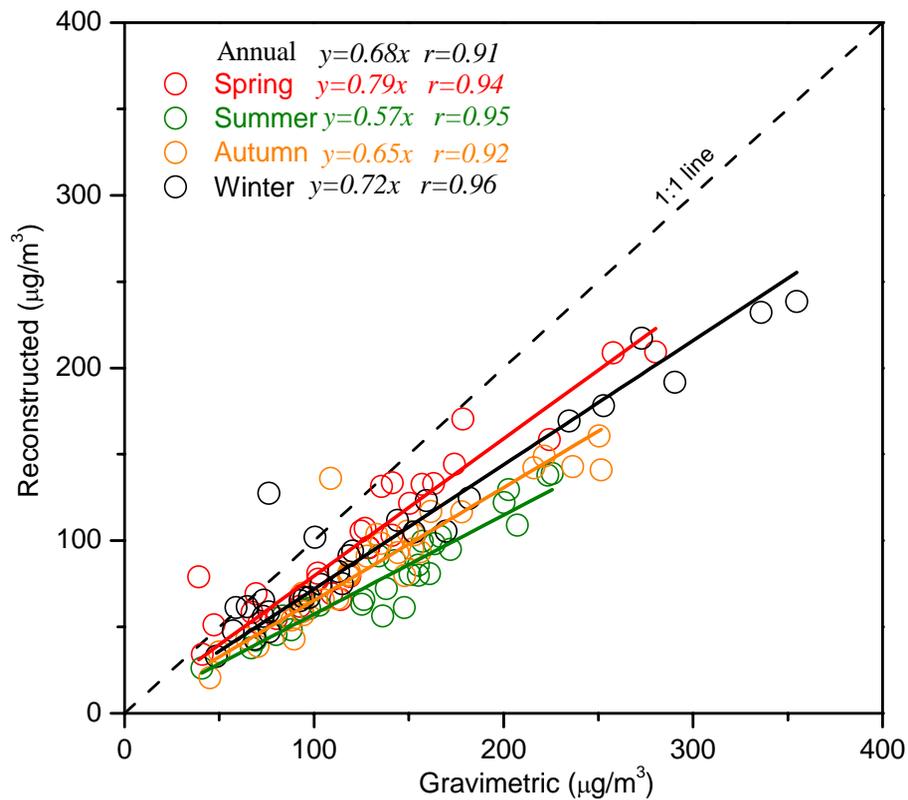
Fig. 6. Scatter plot showing the correlations between the PM$_{2.5}$ mass concentrations reconstructed from the chemical mass balance method and obtained from gravimetric measurement, which are presented on a seasonal basis. Linear regression lines are shown with equations for the four season period, along with the annual case.

Title Page

Abstract | Introduction

Conclusions | References

Tables | Figures

|◄ | ►|

◄ | ►

Back | Close

Full Screen / Esc

Printer-friendly Version

Interactive Discussion
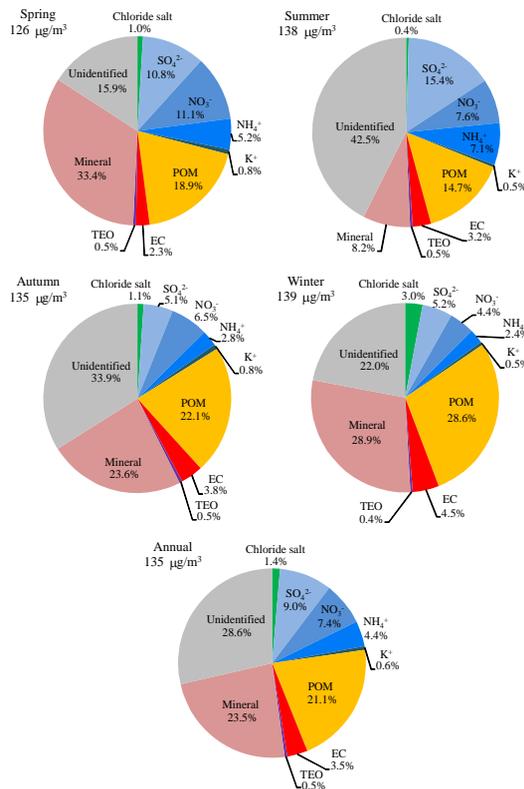
Fig. 7. Pie-charts showing the constructed chemical mass closures for PM$_{2.5}$ in Beijing: **(a)** spring; **(b)** summer; **(c)** autumn; **(d)** winter; and **(e)** annual. The components include mineral dust, secondary aerosol ions (sulfate, nitrate, and ammonium), POM, EC, trace element oxides (TEO), chloride salt, and biomass burning-derived potassium. Other than the identified components, unidentified fractions comprise a significant portion of PM$_{2.5}$.
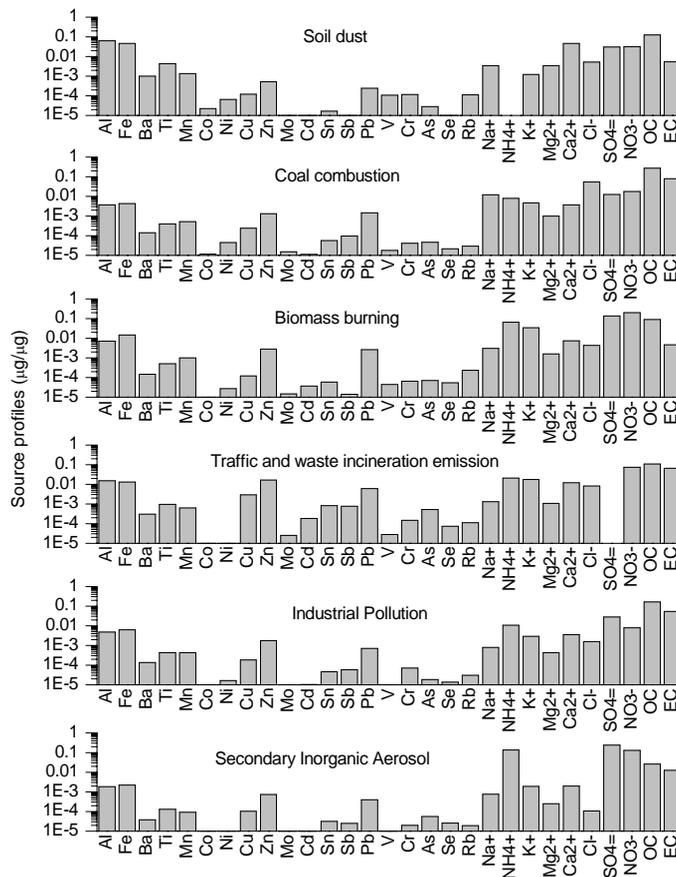
Fig. 8. Profiles of six sources identified from the PMF model, including soil dust, coal combustion, biomass burning, traffic and waste incineration emission, industrial pollution, and secondary inorganic aerosol (from the upper to the lower panels).
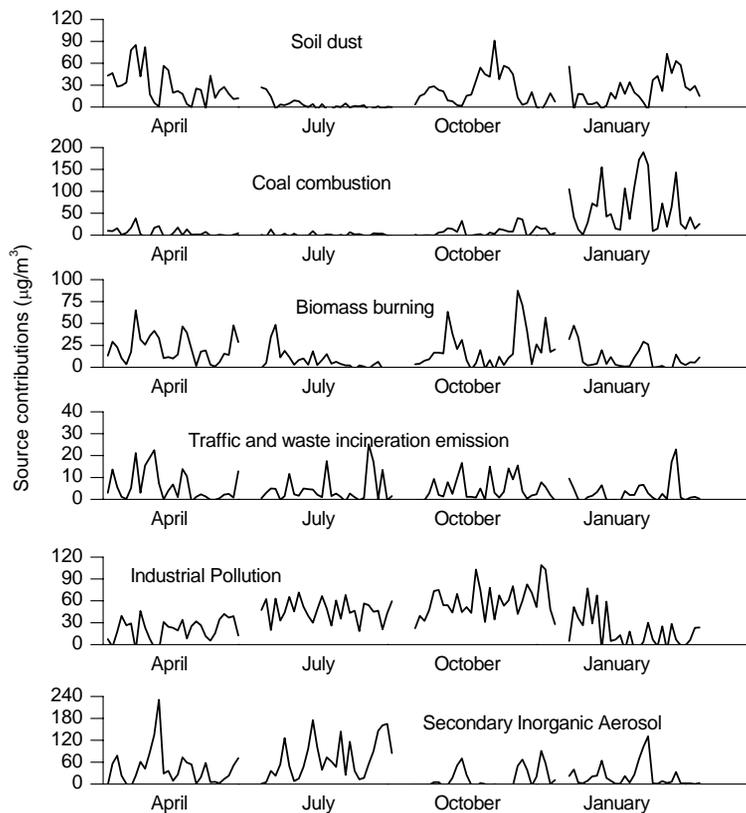
Fig. 9. Time-series of daily contributions from each identified source, including soil dust, coal combustion, biomass burning, traffic and waste incineration emission, industrial pollution, and secondary inorganic aerosol (from the upper to the lower panels) during the study period between April 2009 and January 2010.
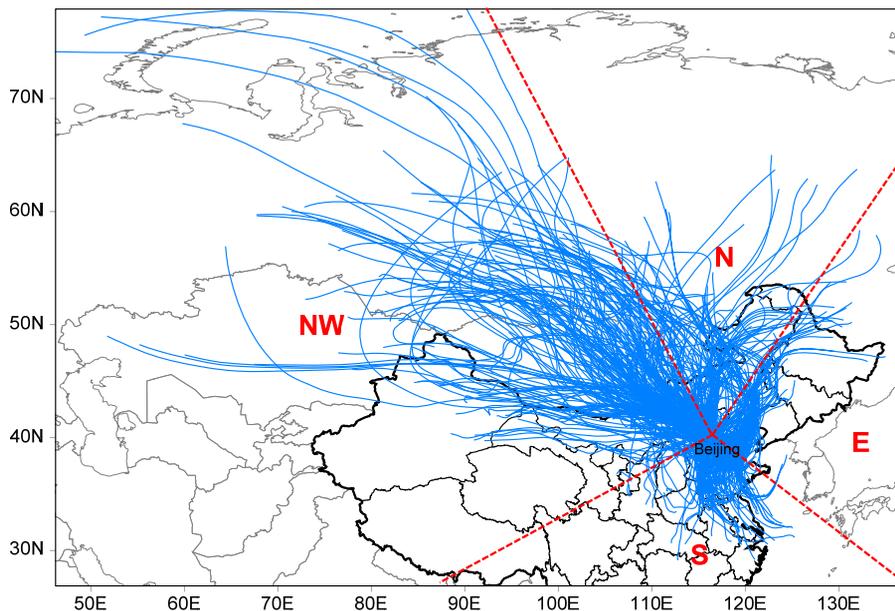
Fig. 10. Analytical results of the 48 h air-mass back trajectories at 100 m elevation during the sampling periods, which were run four times per day. Four regions were defined based on the trajectory clustering results, namely, NW, N, E, and S regions.
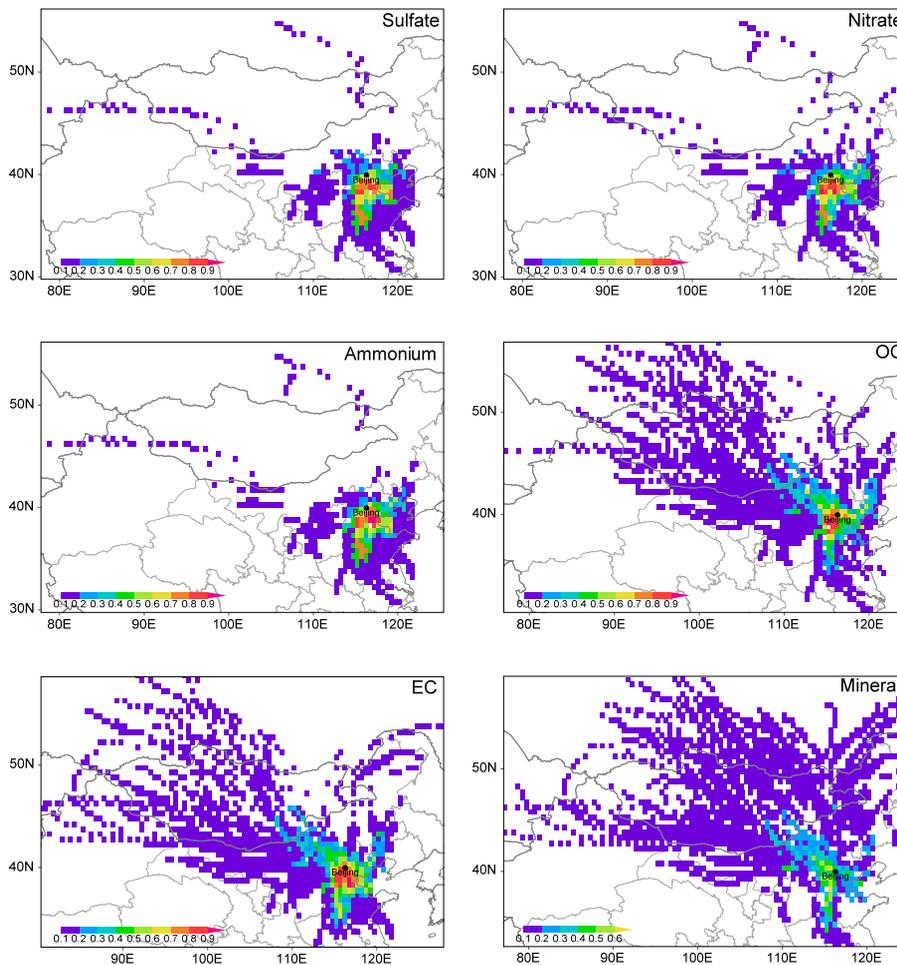
Fig. 11. The PSCF maps for sulfate, nitrate, ammonium, OC, EC, and mineral.